

REVIEW

Open Access

Astronomical adaptive optics: a review



Changhui Rao^{1,2,3*} , Libo Zhong^{1,2}, Youming Guo^{1,2}, Min Li^{1,2}, Lanqiang Zhang^{1,2} and Kai Wei^{1,2,3}

*Correspondence:
chrhao@ioe.ac.cn

¹National Laboratory
on Adaptive Optics, Chengdu,
China

²Institute of Optics
and Electronics, Chinese
Academy of Sciences, Chengdu,
China

³The University of Chinese
Academy of Sciences, Beijing,
China

Abstract

Since the concept of adaptive optics(AO) was proposed in 1953, AO has become an indispensable technology for large aperture ground-based optical telescopes aimed at high resolution observations. This paper provides a comprehensive review of AO progress for large aperture astronomical optical telescopes including both night-time and day-time solar optical telescopes. The recent AO technological advances, such as Laser Guide Star, Deformable Secondary Mirror, Extreme AO, and Multi-Conjugate AO are focused.

Keywords: Adaptive optics, Deformable secondary mirror, Extreme AO, Multi-conjugate AO

Introduction

Adaptive Optics(AO) is the technology that integrates optics, mechanics, electronics, computer technology, and automation and control technology to compensate for optical aberrations that vary with time and space. The concept of AO was derived from astronomy to assist telescopes to overcome the effects of atmospheric turbulence during observations. In 1953, American astronomer Babcock proposed the idea of correcting optical distortion caused by atmospheric turbulence on the ground-based telescopes [1], which is regarded as the origin of AO. However, the idea was initially considered as science fiction due to limited development in optoelectronics and computer science at that time. It was until 1977 that Hardy et al. constructed the first AO system capable of correcting two-dimensional graphics [2]. Since then, due to the military demand for space target observation and high-energy laser weapons, as well as the gradual maturity of precision mechanics, electronics, computer technology and other related technologies, AO technology has rapidly developed over the past 50 years. In October 1989, the European Southern Observatory(ESO) and the National Optical Observatories(NOAO) jointly funded the development of the first civilian AO system named "Come-on" [3]. The system was installed on the 1.52m telescope of the Haute-Provence Observatory in France and achieved diffraction-limited imaging in the $2.2\mu\text{m}$ band. Since then, major economies such as China, the United States, Japan, Europe have conducted research on AO technology, leading to significant achievements. Up to now, all large aperture optical telescopes designed for high resolution imaging in the world have been equipped with AO systems. However, the scientific objectives of large telescopes necessitate AO correction in a large field of view(FOV)(a few arcminutes) and a wide spectral range(visible

to mid-infrared), which poses significant technical challenges. To meet these challenges, multiple AO systems, such as Multi-layer Conjugation AO (MCAO) [4], Multi-object AO(MOAO) [5], Ground Layer AO(GLAO) [6], and different systems have been designed in accordance with different scientific goals. Some of the employed technologies are beyond current technical capabilities and can only be implemented gradually. AO techniques have been developed over the past half century and routinely used in large aperture ground-based optical telescopes for more than 30 years. Although this technique has already been employed in a number of applications, the basic setup and methods have remained the same for the past 50 years. In recent years, AO is experiencing a dramatic boost as a result of the rapid development of artificial intelligence. Nowadays, Machine learning provides improvements in almost every AO-related area. Prominent reviews by experts such as Peter Wizinowich on AO in astronomy [7], and Stefan Hippler on AO for Extremely Large Telescopes [8] provide comprehensive insights. Additionally, Guo & Rao's review focuses on intelligent AO [9], and for a historical perspective on Sodium Laser Guide Stars (LGS), d'Orgeville & Fetzer's 2016 overview and review is available [10].

In this paper, the AO developments for astronomy are introduced. We will pay more attention to recent developments in AO technology, such as LGS, Deformable Secondary Mirror(DSM), Extreme AO(ExAO), and wide field AO. Finally, we describe the developing AO systems at three 30m class extremely large telescopes and two 4m solar telescopes.

The principle of AO

Without any aberration, the wavefront originating from an astronomical object is initially a plane wave before it enters the earth's atmosphere. However, the refractive index of air varies in space and time, affecting the light speed as it passes through the atmosphere and causing distortion of the wavefront [11]. AO technology compensates for these atmospheric effects, allowing ground-based telescopes to achieve their theoretical diffraction-limited resolution. With the use of AO, high angular resolution has become a crucial tool for investigating and comprehending the universe over the past two decades, especially when combined with the world's largest telescopes and state-of-the-art scientific instruments. The concept of AO is illustrated by the simple schematic in Fig. 1. A distorted wavefront enters the telescope and is reflected off by a fast tip-tilt mirror and a deformable mirror(DM). A portion of the light is directed to a wavefront sensor(WFS) to measure the distortion. The motion can be corrected by the fast tip-tilt mirror. The DM applies higher-order corrections, which can be performed by the same mirror if it has enough stroke or is mounted on a fast tip-tilt stage. The result is a corrected wavefront transmitted to the science instrument, such as a high-resolution camera, allowing ground-based telescopes to achieve their theoretical diffraction-limited resolution by compensating for the blurring effects of the earth's atmosphere.

Key technologies in AO system

The key AO technologies, to be discussed next, include: DM, WFS and guide star(GS).

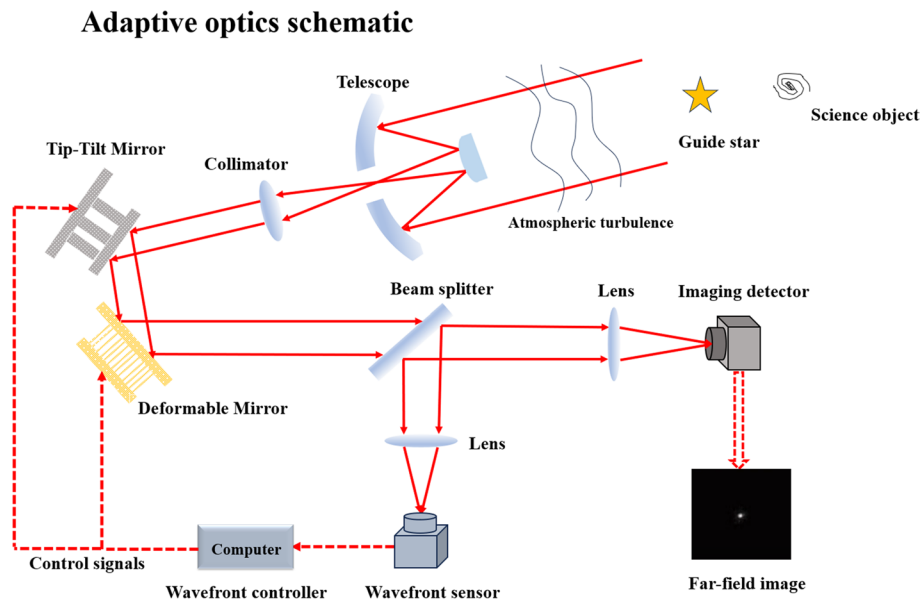


Fig. 1 AO concept. The light from the telescope is reflected off a fast tip-tilt mirror and a DM before being split between the WFS and the science (high-resolution) camera. The image motion and wavefront distortions are computed by the tip-tilt and wavefront control systems and are applied to the tip-tilt and DM, respectively

Deformable mirror

Wavefront correctors change the wavefront of the incident beam, which can be achieved by transmission or reflection, with reflection wavefront correctors being the most commonly used. In addition, wavefront correctors can be divided into two categories: fast tip-tilt mirrors and DM, depending on the form of optical wavefront aberration introduced or compensated for. The fast tip-tilt mirror is used to correct the overall tilt of the wavefront by deflecting the mirror. Its main function is to eliminate jitter in the imaging spot caused by external disturbances such as atmospheric turbulence or device instability, and it requires a response rate ranging from several hundred to several thousand Hz. The remaining wavefronts with relatively complex spatial shapes require to be corrected by DM, whose mirrors are driven by numerous actuators to produce a controlled and complex deformation. Since 1953, when H.W. Babcock first proposed the idea of AO technology [1], the structural form of DM of AO systems has gradually evolved from the initial “Ediophor” oil film model to a variety of mirror structural forms such as flat, spherical or aspheric integral mirrors. A variety of optical devices are available, including piezoelectric, electromagnetic and electrostatic actuators, and reflective and transmissive modes of operation. Below, we will briefly introduce several typical DMs. The schematic diagram of the piezoelectric stacked DM, the MEMS DM, the bimorph DM and the voice-coil motor-driven DM are shown in the Fig. 2.

The piezoelectric stacked DM has a wide application range, characterized by a stable structure, good surface quality, high damage threshold, high resonant frequency of the driver. In recent years, the main development direction is to develop DM with a large number of driving units to meet the needs of large ground-based telescope systems [12–14].

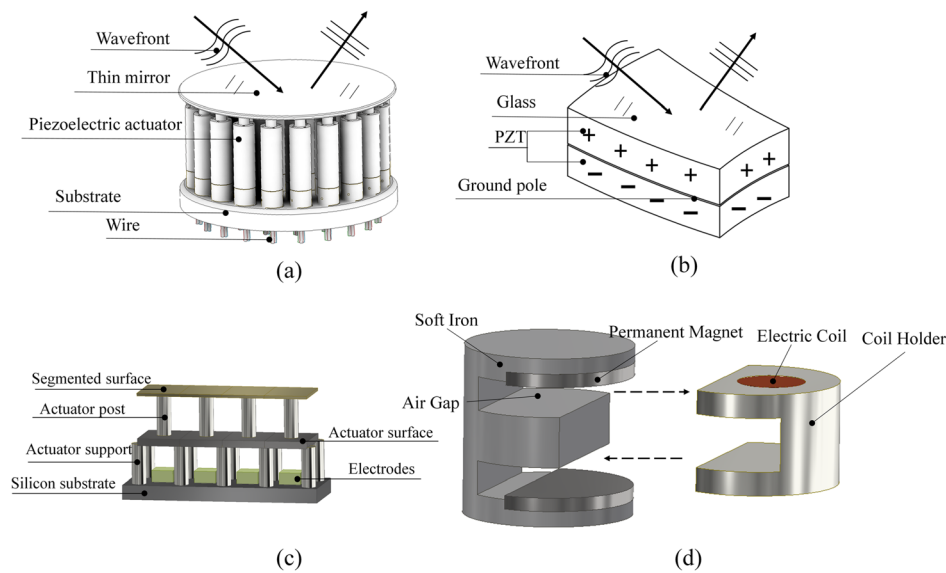


Fig. 2 **a** The Piezoelectric stacked DM, **b** The Bimorph DM, **c** The MEMS DM, **d** The voice-coil motor-driven DM

MEMS DMs are compact, highly integrated, cost-efficient in mass production, and pivotal for the miniaturization and integration of AO systems. Due to the relatively mature technology development in the past, hundred-cell devices have basically achieved commercial applications. In recent years, large-scale multi-cell devices have become the primary focus of technical research direction [15].

The Bimorph DM is an ideal low-order aberration correction device because of its large low-order correction range, high damage threshold and relatively low cost. However, the number and caliber of its units are limited by the manufacturing process, and it is basically aimed at the application of small and medium-sized caliber, 100 units level AO system within 50mm. Recent research has been attentive to expanding the application to large calibers [16–18].

The voice-coil motor-driven DM has a large stroke, can simultaneously correct tilt and high-order errors, and has no rigid connection between the mirror and the driver. It has improved maintainability and strong resistance to driver failure. Most voice-coil DM are used in DSM AO system. It will be an important technical route for the future large-aperture telescope AO system [19–21].

Traditionally, special deformable mirrors (including tip-tilt mirrors) and relay optics are usually installed at the post focus of a telescope, independent of the telescope optics. This configuration results in a complex imaging system with low throughput and high heat dissipation. The concept of DSM integrating the telescope and AO system. The multiple mirror telescope (MMT) was the first DSM-based telescope, following the large binocular telescope (LBT), Magellan telescope (MT) and the UT4 of the very large telescope (VLT). These large-diameter adaptive telescopes were all based on the voice-coil DSMs (VCDSMs). These telescopes have successfully demonstrated the advantages of DSMs, such as high optical throughput, compact volume, and wavefront correction for different foci. In the context of medium-aperture

telescopes, the team from IOE demonstrated the feasibility of piezoelectric DSM (PDSM) for astronomical observation. The structure of the PDSM is much simpler than the VCDSM, eliminating the need for additional position sensors, local electronics, or active thermal control. The detail description of the DSM are summarized at typical AO system section.

Wavefront sensor

Wavefront sensing is one of the three core technologies of AO systems and servers as the basis for wavefront control. According to their underlying operating principles, wavefront sensing techniques can be broadly classified into three categories: intensity-based inverse phase sensing, wavefront slope or curvature-based wavefront sensing and interference-based wavefront sensing. Wavefront sensing techniques applied to AO systems are mainly focused on the first two, as they provide support for high-performance wavefront control through accurate wavefront detection. The Shack Hartmann WFS(SHWFS), Pyramid WFS(PWFS), Curvature WFS(CWFS)are the more commonly used WFS in astronomy. The information of WFS used at typical AO systems are listed at Table 1. The schematic diagram of those WFS are shown at Fig. 3.

By splitting the subaperture, SHWFS achieves the detection direction of the local light field, then the overall wavefront distribution of the input wavefront is obtained by a reconstruction algorithm. The PWFS is developed based on the Foucault knife inspection technique, which has the advantages of high optical energy utilization and high sensitivity, and when used with fast modulator can achieve large dynamic range and highly sensitive wavefront detection, therefore, it is widely used in the field of astronomical observation. In order to achieve wavefront detection, the CWFS is based on the effect of phase distortion on the light intensity during transmission. The process entails focusing

Table 1 The WFS used at typical telescope’s AO system

Telescope	WFS	#Arrays	Frame rate
LBT	PWFS	30 × 30	1000
MagAO-X	PWFS	28 × 28	3630
Subaru	PWFS	50 × 50	3600
Keck	VPWFS and IRPWFS	20 × 20	700
Gemini Planet Imager	PWFS	-	2000
Keck Planet Imager and Characterizer	PWFS	-	1500
GMT	LTAO: SHWFS LGS	6 × 60 × 60	2000
	NGAO: NGS	2 × 92 × 92	
	GLAO: SHWFS	24 × 24	
University of Hawaii 2.2-meter telescope	SHWFS	16 × 16	2000
MMT	SHWFS:	12 × 12	1000
	VPWFS,IRPWFS		
E-ELT	LO: SHWFS	2 × 2	1000
	HO:PWFS		
GTC	SHWFS	20 × 20	2000
VLT	SHWFS	4 × 40 × 40	1000
TMT	NGS: PWFS	-	800
	LGS:SHWFS	6 × 60 × 60	
1.2m Euler Swiss telescope	SHWFS	11 × 11	1800

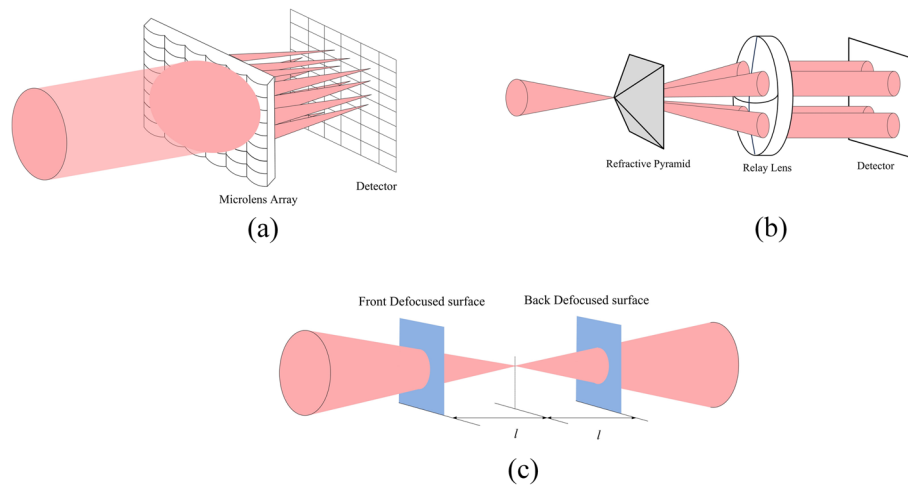


Fig. 3 Schematic drawings of the three main WFS working principles. **(a)** SHWFS, **(b)** PWFS, **(c)** CWFS

the wavefront to be measured through the lens and then to obtain phase information by using the intensity distribution on the two symmetrical out-of-focus surfaces located before and after the focal plane of the lens. As a popular WFS, SHWFS has now achieved detection resolutions of up to 128×128 arrays [22] and is more often used in astronomical applications for mirror error detection in collocated mirrors, such as the collocation of large-aperture telescopes like the Thirty-Meter Telescope (TMT), European Extremely Large Telescope (ELT), Giant Magellan Telescope (GMT) [23, 24]. SHWFS are also usually used at the solar AO system. In solar observation, WFS has to work on low contrast, extended, time-varying objects such as solar granulation. PWFS, on the other hand, has a tendency to replace SHWFS and become the mainstream choice of the WFS at AO system mounted at large-aperture telescope.

As emerging wavefront sensing techniques, deep learning wavefront sensing technology and light field wavefront sensing technology have also drawn the attention of many scholars in recent years, these technologies are expected to overcome many challenges posed by traditional sensing techniques, such as super-resolution and fast high-resolution wavefront recovery. The most representative work is the large-scale 128 cameras array built by Wilburn and Joshi at Stanford University [25], which improves the imaging resolution, dynamic range and other information by taking images of the same scene from different angles to obtain the performance simultaneously, surpassing the capabilities of conventional wavefront detection. In 2005, Ren et al. proposed a super quadratic light field detection method [26], which places an array of microlens in front of the sensor array, thus enabling the camera to capture scenes with different FOV and recover images of each depth of field. This method significantly reduces the size of conventional light field detection equipment and enables the first handheld light field camera. However, the main problem with light field measurement methods using camera arrays and those using microlens arrays is the inability to combine high spatial resolution with high FOV sampling rate, a contradiction that Veeraraghavan resolved by inserting a mask plate into a regular camera [27]. This frequency multiplexing technique converts the image into the frequency domain for acquisition. Marwah et al. at the MIT Media

Lab obtained higher spatial resolution by combining compressed light field acquisition methods [28]. In conclusion, wavefront sensing technology is not only an important part of AO systems, but also a key aspect of many optical detection techniques. It is believed that more efficient, convenient as well as robust wavefront detection techniques will emerge in the next technological development to continuously promote the development of optical manipulation technology.

Guide star

AO systems on telescopes rely on sufficiently bright stars in the sky as GS, enabling the measurement of wavefront aberration caused by the atmosphere for a reasonable correction performance. AO systems use two types of GS: natural guide stars (NGS) and LGS. NGS are astronomical sources which are bright enough, and compact enough, to be used to measure the wavefront. Most often these are stars but angularly small extended objects like planets, moons and asteroids in our own solar system or the bright core of a galaxy (e.g. an active galactic nuclei) can also be used depending on the type of WFS. In the early days, AO systems used bright natural stars, such as Sirius, as GS, called NGS, to produce diffraction-limited correction within the isoplanatic patch. This requirement strongly limits the sky coverage defined as the sky field which can be emitted to create artificial bright stars, called LGS. LGSs are bright and can be produced in any patch of the sky. At present, there are three main types of GS: NGS, Rayleigh LGS, Sodium LGS, as shown in the Fig. 4.

The three-dimensional characteristics of atmospheric turbulence determine that wide FOV imaging observations require multidirectional detection and correction of the aberration introduced by atmospheric turbulence. 3D wavefront sensing requires multiple GSs within the FOV. Due to its brightness and distribution issues, NGSs are difficult

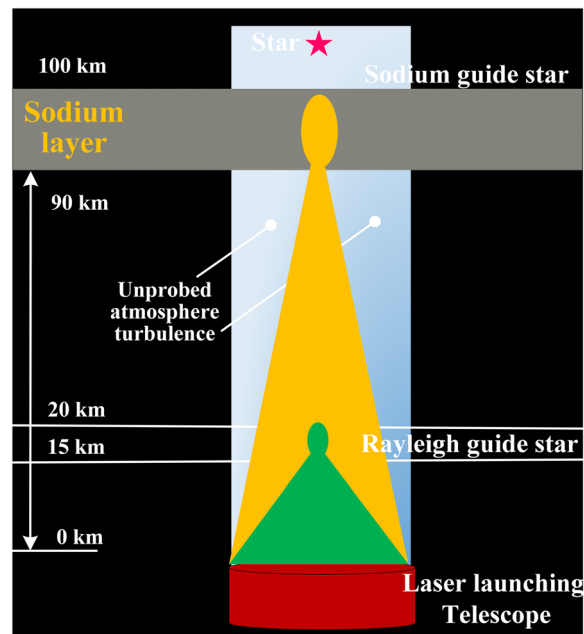


Fig. 4 Guide stars for AO systems

to be used for wavefront detection, so LGS technology is widely used in the field of wide FOV high-resolution imaging.

In 1979, the backscattering signal from atmospheric irregularities was used as a reference beacon for the first time by V P Lukin [29]. In 2019, four Sodium LGSs are successfully implemented by using one small-aperture launching telescope on the 1.8m telescope [30]. Four quasi-continuous-wave(QCW) 20W level beamlets with kHz repetition-rate and hundred μs pulse duration were projected up to the sky successively and produce different LGS constellation on a 40", including linear, parallelogram, rhomboid and square, shown in Fig. 5. Compared with the GeMS, five continuous-wave(CW) LGS system at Gemini South observatory [31], the Rayleigh parasite noise and the fratricide effect on the WFS were eliminated by controlling the pulse synchro system, as a result acquiring higher spatial resolution.

Typical AO systems

The architecture of an AO system determines its performance. According to the different needs for correction capabilities, a variety of AO architectures have been developed, including traditional AO system, ExAO and wide field AO technology. The following is a brief introduction to these AO architectures.

Traditional AO

Traditional AO detects the accumulated wavefront aberrations of atmospheric turbulence in a certain direction of the detection beacon, and sets DM at the pupil surface

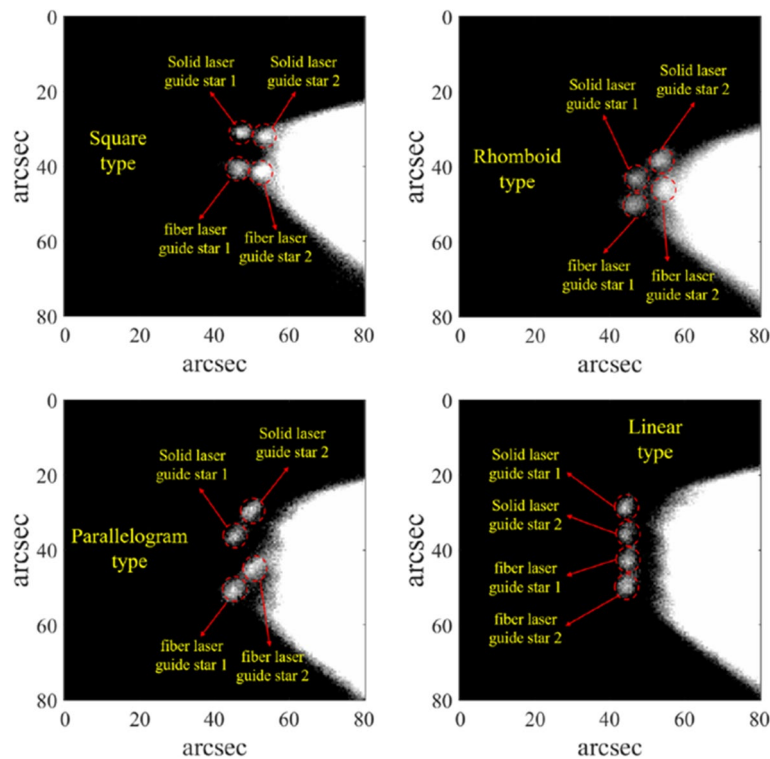


Fig. 5 Images of Sodium LGS clusters and Rayleigh scattering with different configurations

to conjugate and correct the corresponding wavefront aberrations. Due to the anisoplanatism of atmospheric turbulence, the corrected FOV of traditional AO is limited. Only the central FOV has effective correction, whereas the imaging quality of other fields rapidly decreases. In recent years, the unit technology in AO systems has been developed to a certain extent, particularly in the field of GS and the DM. Here we focus on the LGS AO and DSM AO.

LGS AO

In pursuit of higher imaging quality, many large aperture telescopes are equipped with the LGS AO system. Table 2 lists the typical ever-built astronomical LGS AO systems.

The Rayleigh LGS makes use of 532nm green laser-induced incoherent Rayleigh backscatter from air molecules. Rayleigh LGS can be generated at altitudes of up to about 20km [32]. Because of its low height and cone effect, it can only be used to correct the wavefront aberration from the lower atmosphere. Cone effect, also known as the focal anisoplanatism, introduces errors due to the limited altitude of atmospheric sampling and projection effects brought on by conical illumination rather than cylindrical illumination. As a result, the Sodium LGS was later developed [33]. There are many metal atoms in the atmospheric ionosphere at altitudes of 80-105km, among which Sodium atoms are highly abundant and can emit strong Sodium D2 line fluorescence. They are excited by resonance with the corresponding wavelength of 589nm yellow laser. These Sodium atoms will produce strong back fluorescent radiation, which is called Sodium LGS. Because of its high generation height(close to the top of the atmosphere) and high brightness, it can well correct the wavefront distortion caused by the nearly entire atmosphere. Consequently, the Sodium LGS has become an advanced beacon source for the development of AO telescopes.

The earliest Rayleigh LGS AO system experiment was carried out by the US Air Force on a 1.5m telescope built in 1982 at the Starfire Optical Range [34]. The system employed a copper vapor laser with a wavelength of 530nm and a Rayleigh beacon is generated at the height of 10km of which sampling thickness is 2.4km. The University of Illinois Seeing Improvement System(UnISIS) is a LGS AO system operating at the 2.5m telescope at Mount Wilson Observatory. It is the first astronomical system to employ a Rayleigh LGS at 351nm [35, 36]. The system started construction in 1994 and successfully conducted an open loop test in 2002.

During the summer of 1982, that the concept of Sodium LGS created in the Sodium layer at 90km can be used for atmosphere turbulence detection was proposed in the revised version of the Jason reports written by W. Happer [37]. In 1997, a Sodium LGS AO system with turbulence high-order compensation at Shane telescope was conducted by C. E. Max [38]. The Sodium LGS was pumped by a tunable dye laser, which projected 18W of average power with a pulse repetition frequency of 11KHz, the photon return of the Sodium LGS comparable to a natural star of magnitude of 7 in V band. In 2000, the ALFA(AO with a Laser For Astronomy) with Sodium LGS was installed on the 3.5m telescope at Calar Alto, and the first science paper based on Sodium LGS AO for astronomical observation was obtained. Soon afterwards, the Sodium LGS AO system was installed on major 10m class ground based telescopes. First Sodium LGS AO were installed on Keck telescope and won several scientific research achievements. The first

Table 2 The typical LGS AO systems

AO Facility	Tel.D(m)	AO Type	First light	LGS			Laser power (w)	Wavelength (nm)	Manufacturer	WFS		Wavefront corrector	
				Type	No.	Laser type				Type	Actuators	Type	Actuators
Hale-PALM3000	5.1	SCAO	1999/2013	Rayleigh LGS	1	Solid	8	589	Carl Zeiss(PALM)	$64^2 \cdot 32^2 \cdot 16^2 \cdot 8^2$ SH	DM conjugated to 0,780m	241+3388	
LBT-ARGOS	8.4	GLAO	2014	Rayleigh LGS	3+3	Solid	18	532	Innolas	SH	DM	672	
RoboAO	1.5	SCAO	2012	Rayleigh LGS	1	Diode-Pumped	10	355	JDSU	SH	MEMS	12 x 12	
Keck I	10	SCAO	2003/2013	NGS/Sodium LGS	1	Solid	25	589	Lockheed Martin	20 x 20 SH	DM	349	
Keck II		NGAO	2000/2005		6	Dye/Diode-Pumped	12-14	589	Lawrence Livermore/TOPTICA/MPBC				
Gemini-N Altair	8.1	SCAO	2003/2007	NGS/Sodium LGS		CW Solid	12	589	Lockheed Martin	SH	DM	177	
Gemini-S GeMS		MCAO	2013	Sodium LGS	5	CW Solid	50	589	Lockheed Martin	SH	DM conjugated to 0,4,5 and 9 km	293,416 & 208	
VLT NACO	8.2	SCAO	2002/2008	Sodium LGS	4	CW	4	589	A French Consortium (ONERA/ODPLAOG)	14 x 14 or 7 x 7 SH	DM	185	
VLT SINFONI		SCAO	2005	Sodium LGS	4	CW	10	589	MPE (Garching) and MPIA (Heidelberg)	Cur	Dual chip	60	
VLT GRAAL(HAWK-I)		GLAO	2018	Sodium LGS/NGS	4/1	CW Fiber Raman	22	589	TOPTICA	40x40 SH	DSM	1170	
VLT GALACSI(MUSE)		LTAO/GLAO	2016							4 WFS(SH) each with 40 x 40	DM	1170	
Subaru	8.3	SCAO	2007/2011	NGS/Sodium LGS	1	Solid	4.5/6.8	589	Megaopto Co., Ltd.	Curvature	Dual chip	2000	

Table 2 (continued)

AO Facility	Tel.D(m)	AO Type	First light	LGS			WFS			Wavefront corrector	
				Type	No.	Laser type	Laser power (w)	Wavelength (nm)	Manufacturer	Type	Actuators
ShaneAO	3	SCAO	2014	NGS	1	Pluse Fiber	3.5/9	589	Lawrence Livermore National Labs	DM	52+1020
WHT-CANARY	4.2	MOAO/GLAO	2020/2023	NGS/Sodium LGS/Rayleigh LGS	3+4	Solid	20-30	515		DM	52+241
GTCAO	10.4	MCAO	2025	NGS/Sodium LGS	1+3	CW Fiber Raman	20	589	TOPTICA	DM conjugated to 0,9,8 km	21x21(373)
SUBARU-RAVEN	8.3	MOAO	2014	NGS/Sodium LGS	2+1	Solid	4-10	589	Megaopto Co, Ltd.	DM	145+145
LGS-AO	1.8	SCAO	2013/2016	Sodium LGS	1	Solid	27/35	589	Technical Institute of Physics and Chemistry(TICP)	DM	37/61

generation sodium LGS AO system of the twin telescopes of Keck I and Keck II began to run at 2012 and 2004 respectively [39–44]. The Sodium LGS was created by 6 dye laser fabricated by Lawrence Livermore National Laboratory with a power of 12W ~14W, the return signal of the single LGS was comparable with a natural star of a magnitude of 9.5~10.5 at V band ($140\sim55$ photons/s/cm²). The wavefront from the Sodium LGS passing through the earth's atmosphere was analyzed by a SHWFS, the sensing information was feedback to a DM with 349 actuators, and the Strehl Ratio(SR) can be increased up to 0.35. Figure 6 shows that the galaxy at 3.4um compensated by Sodium LGS AO system at Keck II telescope.

A group of astronomers has obtained new data that suggest the universe is expanding more rapidly than previously thought. They used NASA's Hubble Space Telescope(HST) in combination with W. M. Keck Observatory's AO system to observe three gravitationally-lensed systems [45]. This is the first time ground-based AO technology has been used to obtain the Hubble Constant. Figure 7 shows the observation.

Meanwhile, other 8m class telescopes and some 4m class telescopes were installed the Sodium LGS AO system, such as the Subaru telescope [46], the VLT UT4 telescope of ESO [47] and the Shane telescope [48]. In 2016, two AO systems with Sodium LGSs asterism were installed on VLT (Very Large Telescope). GRAAL (HAWK-I) is a GLAO system which imaged at J, H, K band with 7.5arcmin FOV [49, 50]. GALACSI can be operated at both GLAO and LTAO (laser tomography AO) mode [51]. The two AO systems share the common LGS launch system with 4 sodium LGSs. For LTAO, the 4 Sodium LGSs in different sight detected the turbulence, which can be separated beyond the isoplanatic angle, but their beams should still overlap at the highest turbulent layer, the reconstructed volume is then collapsed along the third dimension and finally projected onto a single DM, delivering near diffraction limit across a

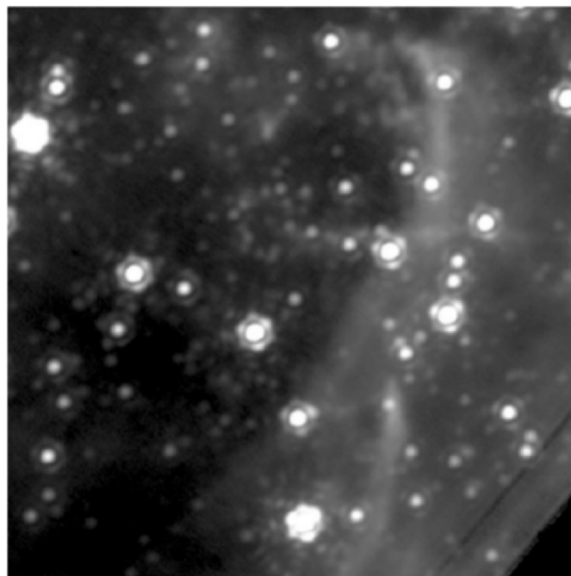


Fig. 6 The photograph of galaxy obtained by Keck II with Sodium LGS AO corrected. The magnitude of the LGS is nearly 14, the SR after compensation is 0.7, the resolution reached to 0.081arcsec (Adapted with permission from [39], copyright the American Astronomical Society)

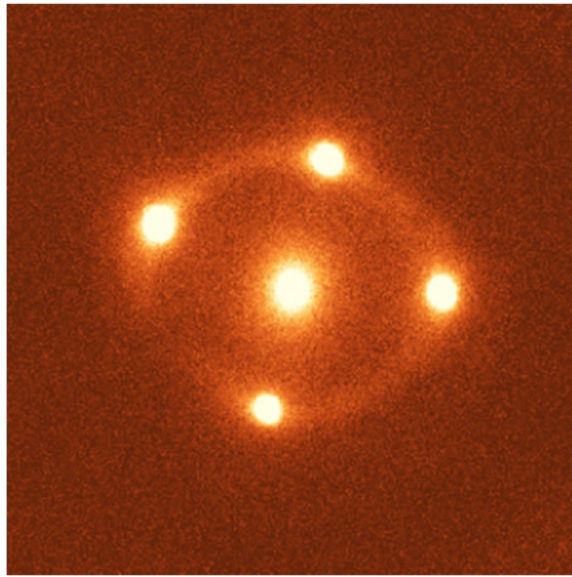


Fig. 7 Keck AO system was used for the first time to obtain the Hubble Constant by observing three gravitationally lensed system, including HE0435-1223 (<https://phys.org/news/2020-09-solar-teles-cope-gregor-unveils-magnetic.html>)

narrow field with a FOV of $7.5''$. 4 copies of 40×40 Shack-Hartmann WFSs track the 4 LGSs which driven secondary deformable mirror compensate the turbulence with 1170 actuators, the SR at 650nm can be reached to 0.1.

Figure 8 presents the results obtained with the VLT/MUSE Integral Field Spectrograph fed by the 4 LGSs and its laser tomography AO module GALACSI in 2019. The unambiguous detection of not one but two $H\alpha$ signals around PDS 70 are discovered. One is at the location of planet b, confirming the presence of an accreting protoplanets and the other one is at the gap edge to the East and is most likely a second, accreting protoplanet [52].

Nowadays, the VLT has made an undisputed impact on observational astronomy. The observations made with the VLT have for the first time revealed the effects predicted by Einstein's general relativity on the motion of a star passing through the extreme gravitational field near the supermassive black hole in the centre of the Milky Way. The 2020 Nobel Prize in Physics was awarded "for the discovery of a supermassive compact object at the centre of our galaxy". Figure 9 presents the observation of the central parts of our Galaxy, the Milky Way, as observed in the near-infrared with the NACO instrument on ESO's VLT (<https://www.eso.org/public/news/eso2017/>). By following the motions of the most central stars over more than 16 years, astronomers were able to determine the mass of the supermassive black hole that lurks there.

The first Sodium LGS asterism MCAO system is GeMS developed at Gemini South telescope [53–57]. It uses five sodium LGSs feeding five SHWFS with 16×16 subapertures to detect the high-order turbulence, driven two DMs which conjugated at 0 and 9km, while the tip-tilt aberrations detected by 3 NGSs and associated NGS WFSs. The GeMS delivers a uniform and close to diffraction limited at near infrared image with an FOV nearly $2'$. The Composite image of MHO 1502 and MHO 2147 obtained with GSAOI/ GeMS in 2021 are shown in Fig. 10 [58].

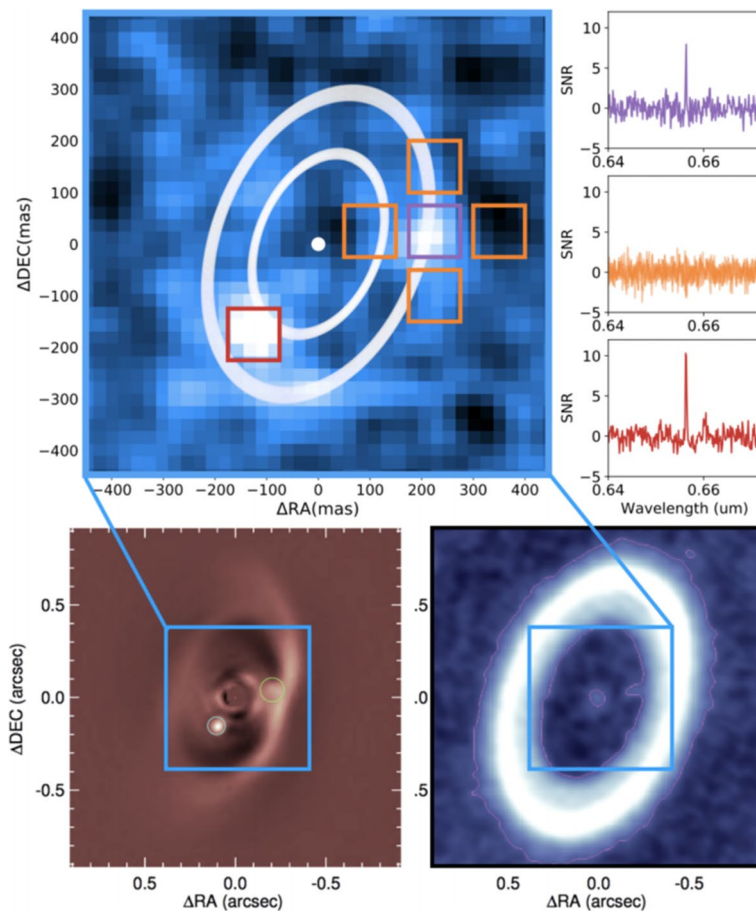


Fig. 8 Top: VLT/MUSE detection ($H\alpha$ SNR map) of both b and c, with to the right, the SNR versus wavelength around the $H\alpha$ line integrated in the corresponding color boxes (red for b and purple for c). The ellipse overlays show the orbital radii for both companions assuming circular Keplerian orbits. Bottom left: PDS 70 b as detected by VLT/SPHERE in K1K2. 18 Planet c is visible though not claimed at the time and called “bridge”. Bottom right: ALMA Cycle 5350.6 GHz continuum image with contours displaying a “spur” roughly at the location of c (Adapted with permission from [52], copyright Cornell University)

Since 2003, the Institute of optics and electronics (IOE) of the Chinese Academy of sciences (CAS) collaborated with Technical Institute of Physics and Chemistry (TIPC), CAS has been actively involved in the development of Sodium laser technology. In 2011, we generated our first LGS with the Magnitude around 8.7 [59], after performing a D2b re-pumping test and installing a compact 37 elements LGS AO system on the 1.8m telescope, and the first LGS AO close-loop result was achieved in early 2014, as shown in Fig. 11.

DSMAO

The concept of DSM, also known as adaptive secondary mirror (ASM) was first proposed by J. M. Beckers in 1989 [60]. By locating the DM in the optical train, the

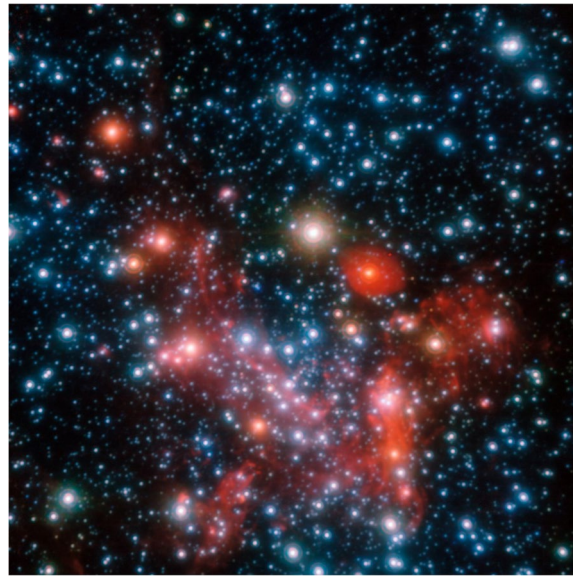


Fig. 9 The image of the Milky Way captured by the VLT NACO instrument

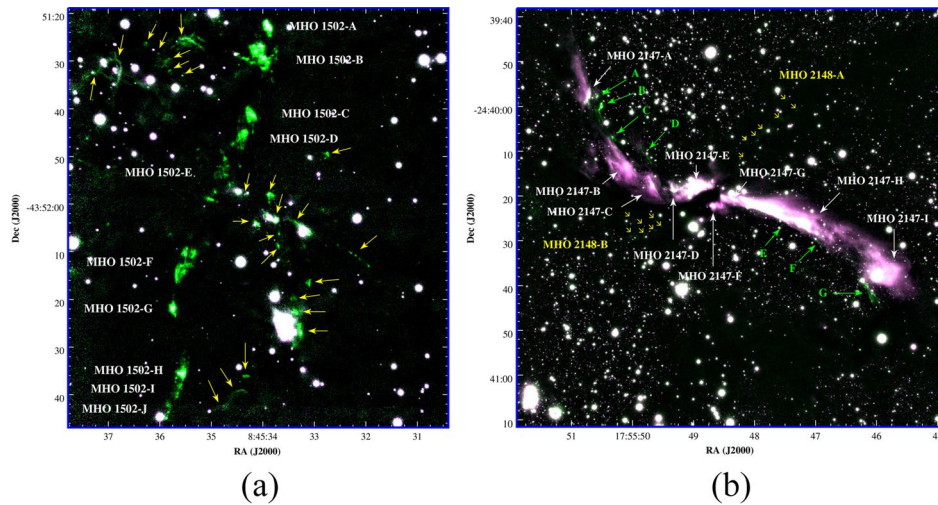


Fig. 10 **a** Composite image of MHO 1502 obtained with GSAOI/GEMINI. The K-band filter is shown in magenta and the H2-band filter in green. The yellow arrows indicate H2 emission adjacent to the MHO 1502 jet, which lie in the field and are unlikely to be associated with this jet. **b** Composite image of MHO 2147 obtained with GSAOI/GEMINI. The K-band filter is in magenta and the H2-band filter is in green. White arrows mark the position of the different knots associated with MHO 2147. Green arrows highlight the knots that seem to belong to another jet (designated Ad-jet) lying adjacent to MHO 2147, while yellow arrows indicate the location of fainter knots linked to the quasi-perpendicular jet (with respect to MHO 2147) MHO 2148

number of optical surfaces is greatly reduced. As a result, lots of advantages can be expected:

- Higher optical throughput, less heat dissipation which would improve the scientific measurements for dim of mid-IR sources [61].

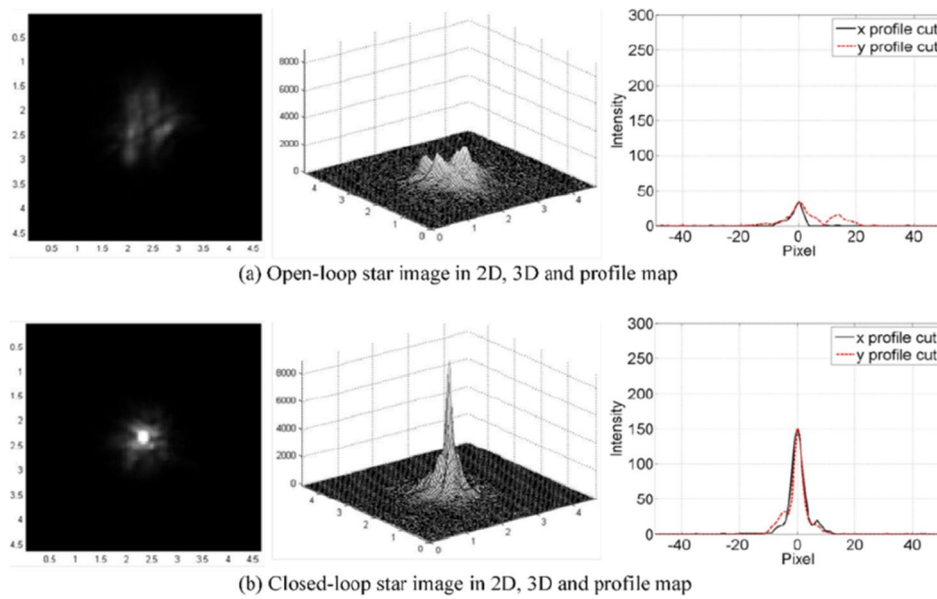


Fig. 11 The open-loop and closed-loop on J Band

- Different optical benches can share the same wavefront correction device [62].
- DSM is the best wavefront correction device for GLAO system of large telescopes especially those with diameters larger than 8m [63].
- Almost no additional polarization is introduced, which plays an important role in the study of polarization of substances such as interstellar dust [64].
- To develop AO with DSM, the focal optical platform only needs an additional WFS, which makes the structure more compact and flexible.

Several 8~10m telescopes [65–67] already have DSMs and two of the 30m class telescopes, GMT [68] and ELT [69] are also working on constructing their own DSMs or DSM-like devices. The ELT has planned to use M4 and M5 as its wavefront correctors, both of which are still located within the optical path of the telescope. Besides of large-aperture telescope, medium-aperture telescopes are also advancing the DSMs [70, 71]. Details about the DSM are described in Table 3.

Table 3 Details about the DSM system at aboard

Telescope	Diam	No. Act.	Act. Pitch in Pupil (m)	Act. Stroke(μm)	Act. Type	Position sensors required	Active cooling required
MMT	642	336	0.30	± 10	VC ^a	✓	✓
Magellan	851	585	0.23	± 20	VC	✓	✓
LBT	911	672	0.28	± 20	VC	✓	✓
VLT	1120	1170	0.21	± 25	VC	✓	✓
UH-88	630	204	0.14	± 15	Electromagnetic hybrid variable reluctance	X	X
1.8m Telescope	320	241	0.13	± 6	Piezoelectric	X	X

^aVoice-coil

Some details about the DSM-based adaptive telescopes are introduced in the following sections.

LBT

In 2010, LBT started using its FLAO system, which consists of 672 units voice-coil DSM(VCDSM) and the PWFS, to conduct high-resolution imaging observations. This successfully pushed the images of high-resolution optical telescope to a new level: the imaging SR of $M_r \sim 9$ target in H-band is up to 0.8. Additionally, it can effectively perform closed-loop corrections with targets as faint as $M_r \sim 17$ as shown in Fig. 12.

Magellan

Magellan uses almost the same VCDSM technology as LBT, but its actuator pitch (mapped to the main mirror 0.23m) is significantly smaller than LBT (mapped to the main mirror 0.28m). This makes Magellan not only have diffraction-limited imaging resolution in the near-IR band, but also performs well in the visible band. Figure 13 shows the observation results of Magellan in the visible band, which is the highest resolution image obtained by the optical telescope at that time [74].

1.8m telescope

Up to now, in the IOE, CAS, two generations of DSMs have been developed. Distinguished from the voice-coil actuators used in large adaptive telescopes such as LBT, Magellan and VLT et al, the DSMs manufactured by IOE are based on piezoelectric actuators. These DSMs, although having smaller strokes than VCDSMs, can effectively match the demands of medium-aperture telescopes(2~4m) since they are less sophisticated than VCDSMs. A 73 units DSM prototype from the first generation was made and then successfully verified on-sky in 2016 on the 1.8m telescope in Lijiang Observatory [71, 75]. Hereafter, to further demonstrate the high-order wavefront correction capability of the piezoelectric DSM, a PDSM-241 was developed which enable the 1.8m telescope to obtain diffraction-limited imaging results [76]. Owing to the effective closed-loop correction of the DSM, high-resolution images were captured by the proposed adaptive telescope. One of the most significant advantages of the adaptive telescope concept is its high optical throughput. To test the performance on faint GS, the open and closed-loop I-band images for a star with a V-magnitude of 8 are shown in Fig. 14. The peak intensity is clearly improved. In general, DSM technology will play a more and more important role in astronomical observation in the future. More degrees of freedom and more robust DSM technology will be the focus of future research in the 30m telescope era.

Extreme adaptive optics

Extreme Adaptive Optics(ExAO) systems are designed to provide highly precise wavefront correction on relatively bright GS, enabling direct imaging of exoplanets around stars [77]. These systems typically operate at faster speeds and have more actuators and sensors than general-purpose AO systems. ExAO systems use a single on-axis star for wavefront sensing. The SR of ExAO systems is generally greater than 80% in the near-IR on bright GS, although image contrast is limited at small angular separations.

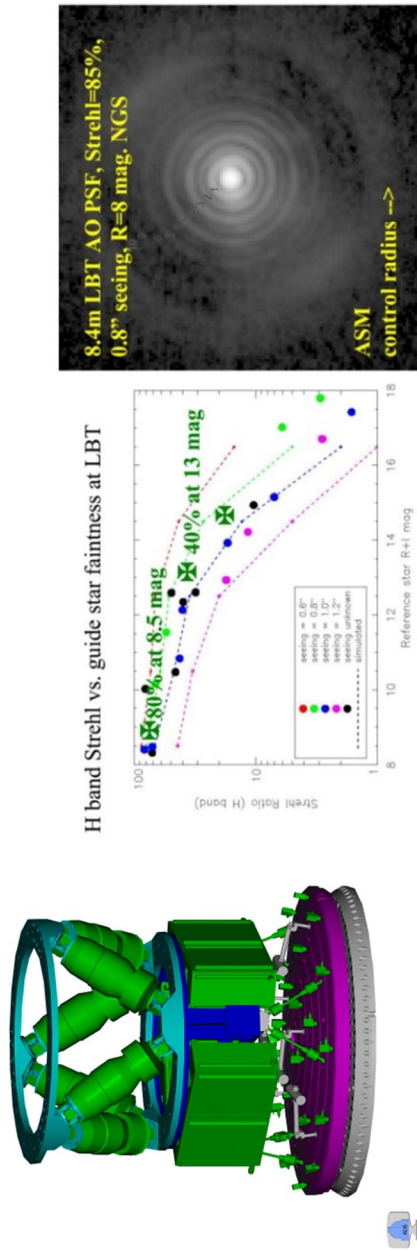


Fig. 12 DSM of LBT (left) [72], relationship between the closed-loop SR and target magnitude in H-band (middle), an example of closed-loop image for a bright star (right) [73]

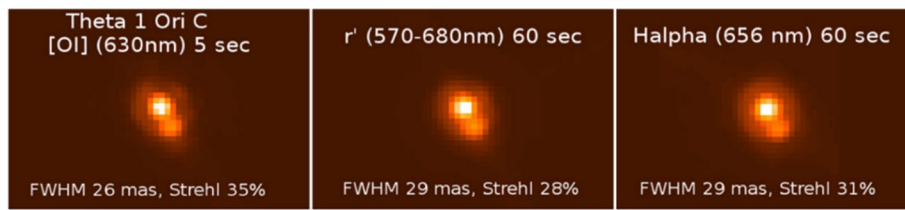


Fig. 13 The observation results of Magellan in the visible band, which is the highest resolution image obtained by the optical telescope at that time [74]

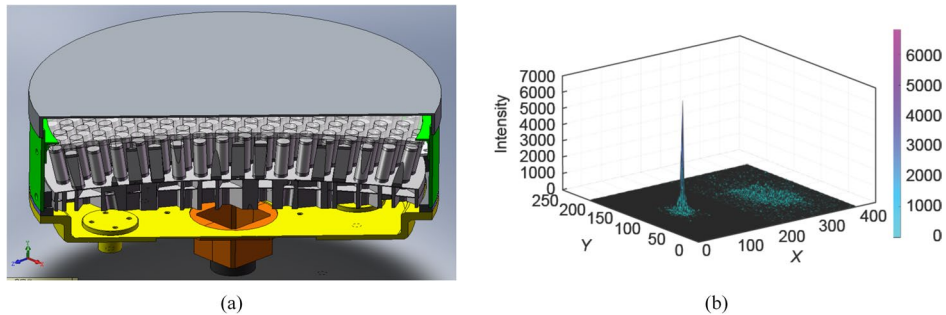


Fig. 14 **a** The sketch of the PDSM-241. **b** Comparison of I-band closed-loop(left) and open-loop(right) image of the star HIP63418(V-magnitude: 8.16)

In 1994, ExAO was first proposed [78]. Following the rapid development of AO systems, several researchers highlighted the potential of ExAO systems combined with coronagraphs to image exoplanets [79, 80]. Around the same time, the first exoplanet detection was announced [81], fueling significant interest in exoplanet imaging techniques.

Since the 21st century, ExAO has experienced rapid development. The globally recognized 10m astronomical telescopes have been equipped with ExAO: including the GEMINI Planetary Imager(GPI) on the Gemini South Telescope and the SPHERE on the VLT of the ESO [82, 83]. Based on ExAO, related technologies for improving the imaging efficiency of exoplanets have been proposed, and test experiments are successively being carried out on a 10m telescope. The hardware innovations of the ExAO system (including scientific imaging cameras, wavefront sensors, coronagraphs and DM) have also enhanced its direct imaging capabilities of exoplanets to a certain extent. The current high-contrast imaging AO system and the corresponding telescope are summarized in Table 4, which includes:

Table 4 The current high-contrast imaging AO system and the corresponding telescope

ExAO	Telescope	Diameters	WFS frequency	DM units	Strehl ratio	Contrast
PALM-3000	Hale	5 m	2 kHz	66 × 66	90%(K-band)	10 ⁻⁵ (@0.5")
GPI	GEMINI	8 m	1 kHz	50 × 50	89%(H-band)	10 ⁻⁷ (@0.75")
SPHERE	VLT	8 m	1.2 kHz	50 × 50	90%	10 ⁻⁶
SCEAO	Subaru	8 m	3.6 kHz	48 × 48	92%	10 ⁻⁵ –10 ⁻⁶

PALM-3000-P1640: High-contrast imaging AO system was installed on the 5m Hale telescope [84]. It uses the ExAO system PALM-3000 and the integrated FOV spectrometer(IFS) in the P1640 system to detect exoplanets. The PALM-3000 system is composed of a 349 units AO system (which is utilized for correcting low-order large-amplitude wavefront errors) and a 3368 units AO system (which is used for correcting high-order small-amplitude wavefront errors) [85]. The corrected SR of PALM-3000 on the bright star in the K-band($I < 7$ magnitude star) is greater than 90%. Nowadays, the team of PALM-3000 has conducted commissioning observations with PALM-3000 and five visible and near-infrared science instruments. In particular, PALM-3000 has quantified the benefit of the speckle suppression technique using P1640, in terms of the faintest companion that can be detected with 5σ confidence as a function of separation from a star. Initial observations achieved a contrast of 10^{-5} at $0.5''$ separation from the star, suitable for detecting luminous sub-stellar companions [85].

GPI: Employed on the GEMINI telescope, which has about 2500 ExAO units [86], the output of GPI is coupled to the coronagraph system and the calibration system, and finally high-contrast imaging is performed by IFS [87, 88]. During first-light observations in 2013, GPI achieved an estimated H band SR of 0.89 and a 5σ contrast of 10^{-6} at $0.75''$ and 10^{-5} at $0.35''$ [82]. Observations of Beta Pictoris clearly detect the planet, Beta Pictoris b, in a single 60s exposure with minimal post processing, as show in Fig. 15.

Using early generation AO systems and cameras, discoveries were exciting but surveys hinted that wide Jovians were rare. Surveys have also revealed a number of brown dwarf companions, highlighting the challenge of distinguishing substellar companion type in direct imaging. The newest ExAO are optimized to look for fainter and/or closer companions. These new instruments have only revealed a few more planets than previous generation instruments. GPI presented the discovery of a brown dwarf companion to the debris disk host star HR 2562 in 2016 [89]. This is the first brown-dwarf-mass object found to reside in the inner hole of a debris disk, offering the possibility to search

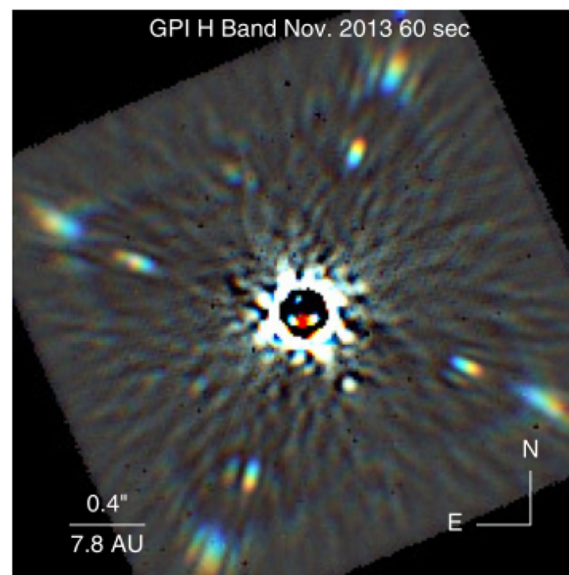


Fig. 15 RGB color composite of a single 60s H band($1.5\text{-}1.8\ \mu\text{m}$) GPI image [82]

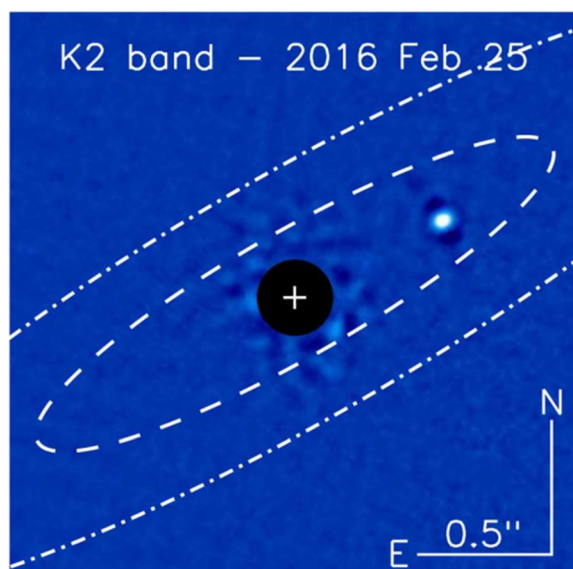


Fig. 16 HR 2562B observed with GPI (Adapted with permission from [89], copyright The American Astronomical Society)

for evidence of formation above the deuterium burning limit in a circum stellar disk, as shown in Fig. 16.

SPHERE: Installed on the VLT telescope, the number of ExAO unit is about 2000 [90]. The high-contrast imaging optical path is divided into 3 parts including [91, 92]: a near-infrared IFS and visible band polarization imaging system ZIMPOL, and an infrared polarization spectrum differential imager (IRDIS) for spectral differential and polarization differential optical channel imaging. In the case of excellent atmospheric seeing, the SR of SPHERE after closed-loop correction is 90% for stars with a magnitude less than 9 in the near-infrared band, with a correction frequency of 1.5 kHz.

The SPHERE system seeks to detect extremely faint sources (giant extra solar planets) in the vicinity of bright stars. Such a challenging goal requires the use of a very-high-order performance AO system, a corona graphic device to cancel out the flux coming from the star itself, and smart focal plane techniques to calibrate any coronagraph imperfections and residual uncorrected turbulent or static wavefronts. The detection limit for the SPHERE instrument is 10^{-6} (i.e, 15 magnitudes between star and the planet) with an aim of around 10^{-8} [93].

New brown dwarfs have also been discovered with SPHERE, several in an interesting class of sources that orbit interior to debris disks. SPHERE used the IRDIS dual-band imager and the IFS integral field spectrograph to acquire high-contrast coronagraphic differential near-infrared images and spectra of the young A2 star HIP 65426 [94]. SPHERE characterized the orbital and atmospheric properties of PDS 70 b in 2018 [95]. SPHERE also obtained high-contrast H-band images of the circum stellar environment of the F5V star HD 206893, known to host a debris disc never detected in scattered light [96]. The images are shown at Fig. 17. The detection of a low-mass companion inside a massive debris disc verifies this system an analog of other young planetary systems such as β Pictoris, HR 8799 or HD 95086 and requires now further characterisation of both components to understand their interactions.

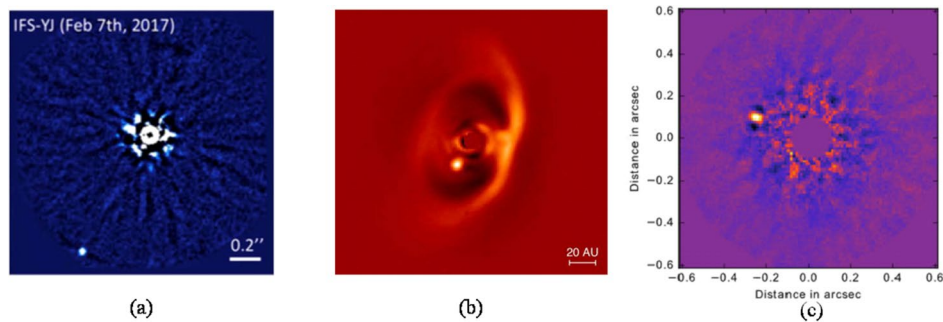


Fig. 17 **a** SPHERE used the IRDIS dual-band imager and the IFS integral field spectrograph to acquire high-contrast coronagraphic differential near-infrared images and spectra of the young A2 star HIP 65426 [94]. **b** SPHERE characterized the orbital and atmospheric properties of PDS 70 b in 2018 [95]. **c** SPHERE H-band coronagraphic image detection of the companion HD 206893 B at 270 mas with a S/N of 14 [96]

SCEXAO: It is installed on the Subaru telescope and uses the original 188-unit AO system, then SCEXAO has been upgraded with a 2000-unit AO system to replace the original imaging system. Finally, SCEXAO is designed to cooperate with various high-contrast imaging systems. SCEXAO can be used as a test platform for the research of high-contrast imaging technology [97, 98]. The primary motivation for such instrumentation is the direct detection of planetary mass companions at contrasts of 10^{-5} - 10^{-6} with respect to the host star, at small angular separations from the host star.

Researchers recently report the new direct imaging discovery of a low-mass companion to the nearby star, HIP 109427, as shown in Fig. 18, with the SCEXAO instrument coupled with the Microwave Kinetic Inductance Detector Exoplanet Camera (MEC) and CHARIS integral field spectrograph [99]. CHARIS data reduced with reference star point spread function (PSF) subtraction yield 1.1-2.4 μm spectra. This work shows the

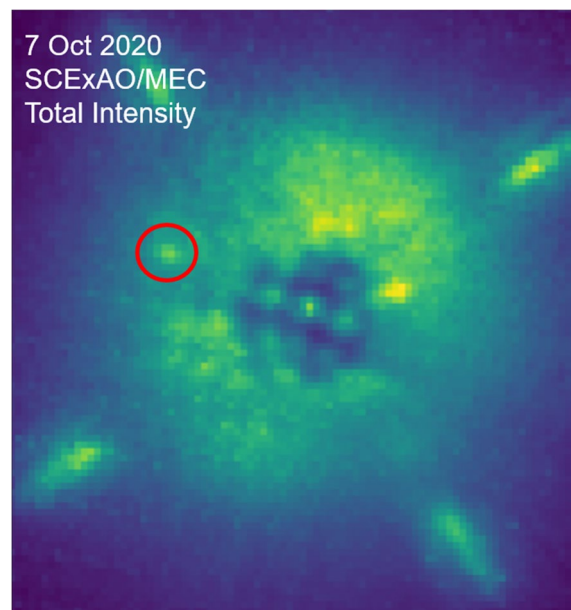


Fig. 18 Total intensity image of HIP 109427 B taken with SCEXAO at Y and J band where the location of the companion has been circled in red (Adapted with permission from [99], copyright The American Astronomical Society)

potential for ExAO systems to utilize speckle statistics to directly image faint companions to nearby stars near the telescope diffraction-limited.

In China, the Nanjing Institute of Astronomical Optics and Technology, CAS achieved innovative results in the research of key technologies for exoplanet detection, such as ground-based high contrast coronal instruments and ExAO [100, 101]. In 2014, the ExAO system developed by the team, as a guest instrument, successfully installed at the ESO 3.6m New Technology Telescope(NTT), successfully completing test observations. This set of ExAO system has obtained diffraction-limited imaging in the near infrared H-band, indicating that it has the ability to be used for scientific imaging and observation of exoplanets.

Wide field AO technology

In astronomical applications, the anisoplanatic error of the atmosphere limits the correction performance of AO system, and the corrected FOV is also constrained, usually in the range of a few arcsec to tens of arcsec at the conventional AO system. This phenomenon comes from that the classic AO system can only detect the accumulated wavefront aberration in one line of sight direction. As the detected FOV expands, light traveling in different line of sight directions will encounter different aberrations, resulting in inconsistent detected aberrations. In this way, the wavefront detected based on a single line of sight direction compensates for other aberrations, and its correction effect will gradually degrade with the expansion of the FOV. Since the 1980s, researchers have been studying how to break through the corrected FOV limitation of existing AO technologies. For different applications, a variety of technical methods to expand the corrected FOV have been developed, which are collectively referred to as wide field AO technology, including MCAO, GLAO, MOAO, etc. MCAO technology was first systematically proposed by J. M. Beckers in 1988 [4]. According to the characteristics of atmospheric turbulence distribution at different heights, MCAO technology proposes layered detection and correction of atmospheric turbulence to realize close to diffraction-limited imaging at a wide FOV. The idea of tomographic detection of atmospheric turbulence in this technology further leads to the proposal of other technologies. In view of the characteristics that atmospheric turbulence is mainly distributed in the ground layer, F. Rigaut proposed GLAO technology [6] in 2001 to detect atmospheric turbulence by tomography, but only correct the turbulence in the ground layer, in order to improve the imaging quality of the system in a larger FOV. Similarly, based on the atmospheric tomography technology, the wavefront information of the FOV surrounding a dim target can be directly reconstructed through the wavefront sensing of the surrounding bright stars, thus to complete high-resolution correction. Such technology is known as MOAO when multiple targets are reconstructed at the same time [102]. MOAO technology enables high-resolution observations of multiple targets within a large FOV, making it ideal for spectroscopic survey observations. A summary of the wide field AO system are listed at Table 5.

With respect to night astronomy, typical test systems include the MCAO verification system MAD on the VLT of the southern European Observatory [103], the MCAO system GeMS [104–106] on the GEMINI South telescope, and the layered MCAO system LINC-NIRVANA [107, 108] of the LBT. After a set of MCAO technology validation tests were completed, the MAD of VLT [109, 110] was taken out of the telescope for

Table 5 A summary of the wide field AO system

#	Telescope	Diameter(m)	AO facility	AO first light time	Imaging band (μm)	GS		WFS		Wavefront corrector		MR	Imaging quality	FOV	AO Type
						Type	Laser	Type	Type	Frame rate	Type				
1	Gemini North	8.1	GNAO	In development	J-, H-, dK band	LGS	Sodium	SH	1kHz	DSM	177	15 < R < 17.5-18.5	SR is 30-50% at K band	NIRI has 22"	MCAO GLAO
2	Gemini South	8.1	GeMS	2013	1-2.5	3N/5LGS	Sodium	SH	800, 400, 200Hz	DM at 0.45 & 9km	293, 416 & 208	16	SR is 15-50% at 1-2.5 μm band	1'	MCAO
3	LBT	8.4	LINC-NIRVANA	After 2016	J, H, K	NGS	n/a	PWFS	1kHz	DSM DM	672 349	10-18	full 23m diffraction-limited resolution	10'x10"	MCAO
4	UH telescope	2.2	ARGOS GLAO Imaka	2015 TBA	1.2-10 JH band 0.6-1	LGS NGS	Rayleigh n/a	SH SH	0.1-1kHz 180Hz	DSM curvature DM	672 36	18-18.5 Expected 26	SR40% at K band FWHM is 0.56" at 0.7 μm band, FWHM is 0.43" at 1.2 μm band, FWHM ~0.3" at visible wavelength within 1 degree FOV.	4'x4' 24'x18'	GLAO GLAO
5	SOAR	4.2	SAM	2013	0.4-1	LGS	Rayleigh	10x10 SH	478Hz	Curvature	60	18	0.6 at 633nm	184'x184"	GLAO

Table 5 (continued)

#	Telescope	Diameter(m)	AO facility	AO first light time	Imaging band (μm)	GS		WFS		Wavefront corrector		MR	Imaging quality	FOV	AO Type
						Type	Laser	Type	Type	Frame rate	Type				
6	VLT	8.2	MAD (Demonstrator)	2008	2-2.5	NGS	n/a	SH or Pyramid	400Hz	Bimorph at 0.8 & 8.5km	2x60	10-14	15 %-30% H and Ks band	2x2K band	MCAO
			ERIS	2016	0.589-2.2	LGS NGS+4LGS	Sodium	SH Pyra-mid	1.0 kHz	DSM	1170	MR< 17 star	GALACSI LTAO delivers SR larger than 10% at 650 nm; NEAR AO module will have to deliver corrected SR at 10.5 μm larger than 97% SR of 15% in V band in a 30" diameter FOV. For LGS wave-front sensing with visible NGS; SR> 60% (MR=12), SR> 55% (MR=17), SR> 35% (MR=19)	2.5"	GLAO TLAO SCAO

Table 5 (continued)

#	Telescope	Diameter(m)	AO facility	AO first light time	Imaging band (μm)	GS		WFS		Wavefront corrector		MR	Imaging quality	FOV	AO Type
						Type	Laser	Type	Type	Frame rate	Type				
7	GTC	10.4	GTCMCAO	2023	1.0-2.5 K	3 LGS	Sodium	3 SH	500Hz	2 DM	373	6-15	SR>=0.65 at 2.2 micron for a bright NGS on axis; SR>=0.1 at 2.2 micron for a faint tip-tilt star brighter than 18 mag	40"x40"	GLAO MCAO
8	GST	1.6	Clear	2016				MD-WFS	1380Hz	3 DM	357.357.357			53"	GLAO. MCAO
9	NVST	1		2022				2 MD-WFSs	1500Hz	3 DM	151.313.373			60"	GLAO. MCAO

laboratory testing. Its GLAO system is now in the development stage [111]. Exemplary GLAO performance at the VLT with Sodium LGSs was shown at Fig. 19. For the MCAO system, MAD utilizes layer-oriented and star-oriented modes for the tomographic reconstruction process. In the layer-oriented process, the PWFS is employed for wavefront detection, with each layer corresponding to a WFS. However, the significant correction improvements are achieved in the star-oriented mode, where each WFS observe a GS. This mode use three 8×8 SHWFSs and two DMs conjugated at 0 and 8.5 km. MAD significantly expands the FOV to 2', achieving a FWHM of 100 mas under seeing conditions of 0.7-1.2". Meanwhile, MAD reaches a maximum SR of 40% in the Ks band, ensuring good field uniformity at approximately 26%.

GeMS on GEMINI South is the first MCAO system put into routine observation and operation. It uses five LGSs and five 16×16 SHWFSs arranged to measure the distorted wavefront. The system employs two DMs that are conjugated at the heights of 0 and 9 km, respectively [31]. GeMS was first tested in observation in 2012 and has since continued to operate.

Since the photon return from the LGS is two to three times less than expected design, ideal photon counts are achievable only when sodium abundance is relatively high, making it challenging for the WFS to measure atmospheric turbulence accurately. This results in a lower SNR for the system. Nevertheless, with the assistance of the LGS, GeMS still expand the FOV to 85". And in the H-band, a significantly improved FWHM of 80 mas can be achieved. LINC-NIRVANA uses the telescope's DSM for ground layer correction. It can access up to 12 NGSs to obtain a FOV of 6'. The high-altitude DM is conjugated at 7.1 km and corresponds to up to 8 NGSs, the FOV at this time is 2'. The system has verified that the ground layer correction module can double the accuracy of FWHM.

Wide field AO system requires multiple GSs for three-dimensional wavefront detection. Targets such as sunspots and granulations on the surface of the sun can be used as GSs. Therefore, the research on wide field AO technology for solar observation has natural advantages. After 2000, German and American scientists successively carried out MCAO technology experiments on 70cm aperture solar telescope VTT [112, 113]



Fig. 19 The VLT view of the planetary nebula NGC 6563 without GLAO correction(left) and with GLAO correction using 4 sodium LGSs(right). The FOV is 1.01'×1.03' [111]

and 76cm aperture solar telescope DST [114], and achieved preliminary experimental results. VTT employs three DMs conjugated at heights of 0 km, 8 km, and 25 km, respectively. The multi direction Shack-Hartmann WFS(MD-WFS) for high-altitude atmospheric correction designs six subapertures, each with a detection field of $68'' \times 68''$. Within each subaperture, 19 guide regions are selected, simultaneously detecting wavefront aberrations along 19 line-of-sight directions. In comparison to traditional AO systems, its correction field is expanded by approximately three times. On the other hand, DST's MD-WFS consists of 25 effective subapertures, with each subaperture selecting 3 to 4 guide regions. The conjugate height of the high-altitude correction DM is adjustable in the range of 2 to 10 km. By achieving a correction image residual jitter variance of less than $0.01''$, a correction field of $42''$ is obtained.

Subsequently, the development of MCAO system was carried out for German 1.5m aperture solar telescope GREGOR [115] and American 1.6m aperture solar telescope GST [116, 117]. Due to the problem of telescope secondary mirror, the advances of MCAO system of GREGOR was slow, while GST's MCAO system was successfully tested and observed in 2017 [118]. The first-phase experimental system mainly adopts the conventional solar MCAO architecture, with one on-axis WFS and one MD-WFS. The MD-WFS utilizes 19 subapertures, and within a detection field of $85'' \times 85''$, a maximum of 19 guide regions can be selected. Three DMs are conjugated at heights of 0 km, 2-5 km, and 6-9 km, respectively. However, the correction consistency within the large FOV is poor at this stage. In the upgrade of the second-phase system, Clear plans to use one MD-WFS for wavefront sensing while simultaneously controlling three deformable mirrors for correction. The MD-WFS has an array of 12×12 subapertures, with each subaperture corresponding to 9 guide regions. This system achieves an ideal $53''$ correction field, and the imaging consistency is significantly better than the previous experimental system. Figure 20 shows the closed-loop observation results of solar granulations and sunspots under different system operating modes during GST's first light.

The theoretical research of wide field AO in China started early. In the 1990s, University of Science and Technology Beijing conducted MCAO theoretical research [119, 120]. In the new century, many domestic institutes, including the IOE, the University of Electronic Science and technology of China(UESTC), the Changchun Institute of Optics, fine Mechanics and Physics(CIOMP), CAS and other institutes, have carried out theoretical research and simulation analysis [121–127]. Nanjing Institute of Astronomical Optics and Technology, CAS has also done some research on the GLAO and MCAO system [128–131]. Among them, IOE has successively developed GLAO and MCAO prototype systems based on the 1m NVST platform of Yunnan Observatory to comprehensively study and verify the wide field AO technology [132–134] as shown at Fig. 21. Since 2018, with funding from the National Natural Science Foundation of China's major scientific research instrument project, the team at IOE, CAS has been working on a set of tested MCAO systems for NVST. The system includes three working modes: traditional AO, GLAO and MCAO.

The conventional solar MCAO system mainly consists of a traditional AO and high-altitude correction loop. This system architecture exhibits a phenomenon where the correction effect in the middle of is significant, while the surrounding areas show poorer correction. The team from IOE,CAS proposed a system

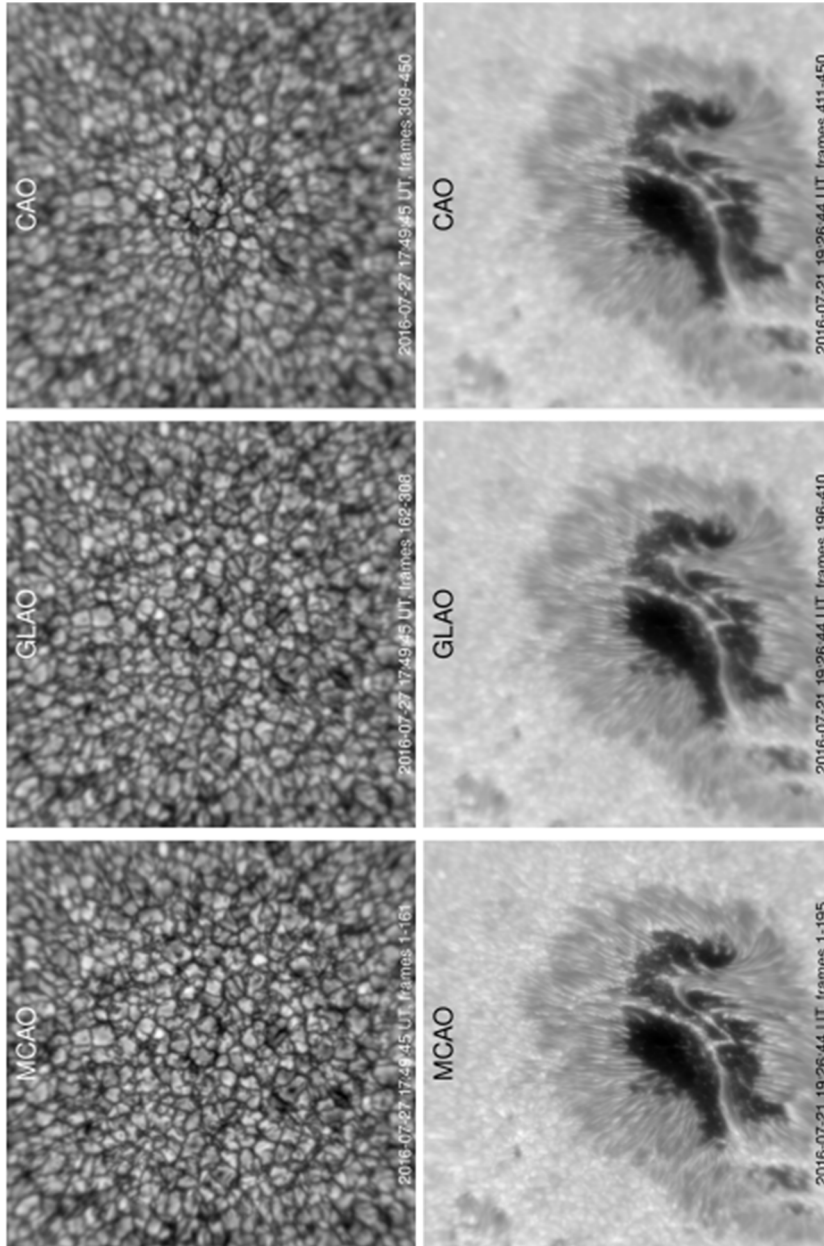


Fig. 20 The closed-loop solar images of MCAO, GLAO and CAO systems obtained by the "Clear" on the GST [118]

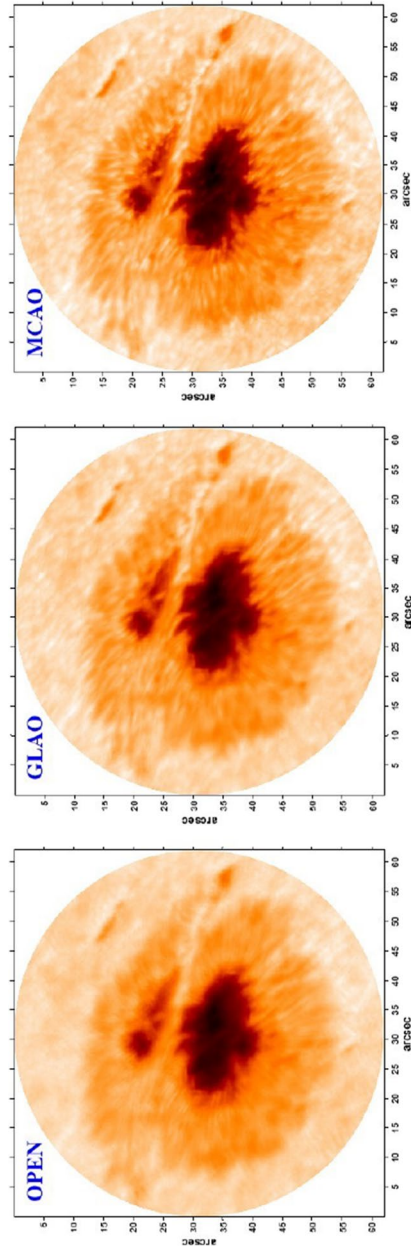


Fig. 21 The TIO band images observed from different operation mode at NOAA 12683. left: open loop image, middle: GLAO image, right: MCAO image

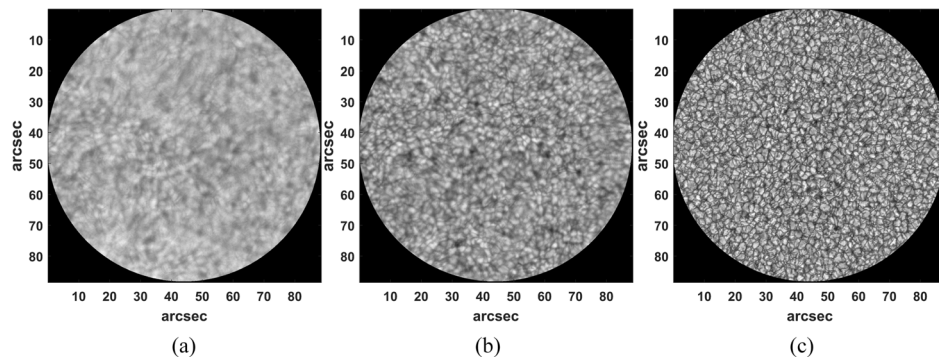


Fig. 22 Short-exposure images of sunspots before (a) and after GLAO correction (b) and speckle reconstruction images (c)

architecture that utilizes ground layer correction along with high-altitude correction. The goal is to improve the consistency of the entire field's correction performance. The GLAO module of this system employs a wavefront sensor with 9×8 subapertures, extracting $9(3 \times 3)$ guide regions for multi-directional wavefront sensing. The high-altitude correction module utilizes a 9×9 WFS, 19 GSs, and a detection FOV of $42'' \times 37''$. At present, GLAO has been put into observational operation [135]. The observations of granulations are shown at Fig. 22. The MCAO is undergoing further commissioning.

The first verification system of MOAO is CANARY installed on the 4.2m telescope WHT [136]. It consists of 8×8 piezoelectric laminated DM(conjugate with pupil) and a high-speed tip-tilt mirror. Since MOAO is an open-loop control system, the system includes four WFSs, three of which are used for atmospheric turbulence tomography and the fourth is used to detect the corrected wavefront. In addition, Subaru Telescope is also carrying out MOAO technology research [137] and developed the demonstration system Raven [138, 139], which has been placed under trial observation. The system can work in three AO modes: traditional AO, GLAO and MOAO [5].

Typical AO applications

Night-time astronomical AO system

For hundreds of years, astronomers have been looking forward to solving the problem of atmospheric turbulence interfering with astronomical observation. As mentioned above, the “Come-On” project started by the ESO in 1985 is the earliest astronomical AO program in the world. Its goal is to provide diffraction-limited resolution imaging technology for ESO's 8.2m VLT telescope [3]. At April 1989, The AO corrected astronomical target image is obtained for the first time at Haute-Provence Observatory in France by using 19 units DM and SHWFS. This is the first step of “Come-On” project [140]. Subsequently, from December 1992 to April 1993, high-resolution imaging of astronomical targets in the infrared band was achieved with 52 units DM and 32 subapertures Hartmann sensor on the 3.6m NTT [141]. Following those early successes, observatories in various countries started AO research one after another. French astronomer Roddier proposed a new concept of detecting wavefront with curvature sensor and correcting

wavefront with double sheet DM [142], so as to realized astronomical target correction on the 3.6m aperture CFHT telescope in Hawaii in June 1992. After the initial breakthrough of astronomical AO, in the early 1990s, the U.S. military began to decrypt its AO technology, and most large telescopes in the world have established teams to develop AO systems. At that time, a number of large telescopes of 8m ~ 10m level, such as Keck [143], VLT [92], Subaru [144], Gemini [31], etc., are eager to equip with AO system, which bring the great development of AO system. A summary of the developed AO systems and properties in the night-time astronomical telescopes above 2m class up to 2021 was listed at Table 6.

The research on AO started early in China. The IOE, CAS began AO research in 1979, set up the AO research laboratory in 1980, and independently established the technical basis of AO for more than 40 years [145]. In 1982, China developed its first DM: a 7 units piezoelectric DM. At present, more than 10 sets of ground-based high-resolution observation AO systems for night-time astronomy have been successfully accomplished. In 1990, a set of 21-element AO system was developed for 1.2m telescope at Yunnan Observatory [146], in which the central aperture with 375mm diameter was used. In 1996, a 21-element AO system had been built and installed at the 2.16m telescope of Beijing Astronomical Observatory for high-resolution observation in K band [147, 148]. A 61-element AO system at the 1.2m telescope of Yunnan Astronomical Observatory had also been constructed for observation in visible band in 2000 [149, 150], then this system was upgraded in 2004 [151]. In 2009, a 127-element AO system had been developed for 1.8m telescope [152, 153]. In 2020, the first light on 4m telescope with 913-element AO system has been achieved. During this time, Nanjing Institute of Astronomical Optics and Technology, CAS has also carried out some research on ExAO system [100, 101, 154] and MCAO techniques. The CIOMP conducted some research on wavefront sensing and correction. Taking the advantage of the tens of thousands of pixels of liquid crystal correctors, the team achieved a breakthrough in the key technology of liquid crystal AO system for large aperture visible light imaging telescopes [155].

With the increase of the telescope aperture, the AO system encounters several difficulties: the quantity of wavefront corrector units is greatly increased, the CCD for wavefront detection is developing to large-scale, high-speed, low noise and high quantum efficiency, the processing capacity of digital wavefront processor is significantly improved, and Na beacon is widely used. In the 21st century, the extremely large astronomical telescope program with an aperture of 30m ~ 40m has been launched. Currently, three extremely large astronomical telescopes are under design, namely TMT [156], ELT [157], GMT [158]. The technologies to be solved in the AO system of super large telescope include: tens of thousands to 100000 units DM (piezoelectric and MEMS), DSM, tens of thousands to 100000 subapertures SHWFS and its high-speed, low-noise and high quantum efficiency CCD detector (long strip image element sub array in different directions is required), high-speed real-time wavefront control computer, 150W Na laser, etc. Some of the techniques have been developed and applied in the AO system, especially the LGS and the DSM techniques.

Table 6 A summary of the developed AO systems and their properties in the night-time astronomical telescopes above 2m class up to 2021

#	Telescope	Diameter(m)	AO facility	AO first light time	Imaging band (μm)	GS		WFS		Frame rate	Wavefront corrector		Magnitude	SR ^a	FOV	AO Type
						Type	Laser	Type	Type		Type	# Actuators				
1	CFHT	3.6	AO	1997	0.7-2.5	NGS	n/a	Curvature	2kHz		Bimorph	19	17	20%@1.25 μm , 60%@2.2 μm	1-2"	SCAO
2	Gemini North	8.1	Altair	2005/2008	1-5	N/LGS	Sodium	SH	1kHz		DM	177	15 R17.5 -18.5	90%@K band (2.2 μm)	22"	NIRI has SCAO
3	Gemini South	7.9	NICI	2008	1-5	NGS	n/a	Curvature	800Hz		Bimorph	85	13-16	5%@1 μm m, FWHM of APDs about two times the diffraction- limited	2x2	SCAO
4	Keck1	10	LGS AO	2003/2013	1-2.5	N/LGS	Sodium	20x20 SH			DM	349		MR ² =10-16, 34-37%	5'x5"	LGS AO
	keck 2		KAPA	2023	1.5-4.5	N/LGS	Sodium	SH Pyramid	1kHz		DM, MEMS DM	349	10-18	16-82%@1.5- 4.5 μm	nearly 100% of the night sky	NGAO
5	LBTx-2	8.4	FLAO	2013	1-5	NGS	n/a	Pyramid	1kHz		DSM	672	10-18	>60%@Hband, MR > 12	15"x 15"	SCAO
6	The Lick Observatory 3m telescope	3	Lick AO to Shane AO	2004	1.1-2.5	N/LGS	Sodium	SH	1kHz		DM to DM+MEMS	60 to 52+1020	11-17	approximately 20" 0.7 to 1.0 μm	70%@ 0.7 to 1.0 μm	SCAO
7	Megellan	6.5	MagAO	2013	0.6-5.3	NGS	n/a	Pyramid	105-1000Hz		DSM	564	1-15	(MR~ 8) 30%- 80%@H band, (MR~ 13) 13%- 40%@H band		SCAO

Table 6 (continued)

#	Telescope	Diameter(m)	AO facility	AO first light time	Imaging band (μm)	GS		WFS		Wavefront corrector		Magnitude	SR ^a	FOV	AO Type
						Type	Laser	Type	Frame rate	Type	# Actuators				
13	GTC	10.4	GTCAO	2021	1-2.5	NGS	n/a	SH	500Hz	DM	373	6-15	SR \geq 0.65 at 2.2 micron for a bright NGS on axis SR \geq 0.1 at 2.2 micron for a faint NGS(MR=14.5)	1.5'	SCAO
14	Auxiliary Telescopes	1.8	NAOMI	2018	0.45-0.9	NGS	n/a	SH	500Hz,100Hz,50Hz	DM	241	13-14	47%@H band	6'x6"	low order AO

^a SR Strehl ratio

^b MR Magnitude range

^c vis Visible band

^d NIR Near infrared band

Solar AO system

Solar activity is the source of space weather. Solar flares, coronal mass ejections and other active regions show large-scale eruptions in the coronal layer, but their energy accumulation, acceleration and triggering are rooted in the lower and smaller chromosphere and photosphere [159–161]. The ground-based large aperture solar telescope is still the best choice to study the sun's fine structure and its active regions. The increasingly mature AO technology ensures the high-resolution observation of the ground-based telescope near the diffraction-limited [162, 163]. At present, the solar AO system has become the standard configuration of ground-based large aperture solar telescopes [164, 165]. Almost all solar telescopes with an aperture of more than 1m are equipped with solar AO system. At the same time, the National Solar Observatory(NSO) [166], the Big Bear Solar Observatory(BBSO) [167, 168], the German Institute of solar physics(KIS) and the National Institute of astrophysics of Spain are all carrying out research on solar AO technology and system development.

In terms of fundamental architecture solar AO systems are quite similar to night-time AO systems. However, compared to night-time AO, solar AO faces a variety of different challenges, and in some aspects, solar AO systems are technically more difficult to implement than night-time AO. The primary challenges come from the poor and time varying daytime seeing, and the fact that solar astronomers mostly observe at visible wavelengths(down to 380nm), and the WFS in the AO system. Due to heating of the ground by direct sunlight, the near-ground turbulence layer is much stronger during the day and typical Fried parameters are of order 10cm(500nm) at an excellent site and at a typical telescope height of 20 - 40m above ground. Despite the solar telescopes relatively small(compared to night-time telescopes) apertures, solar AO systems need a lot of correction elements since daytime turbulence conditions are worse and a lot of science is done at visible band wavelength. The solar AO systems must achieve a very high closed loop bandwidth because of the limited value of r_0 at visible wavelengths and with daytime seeing conditions. Another challenge for solar AO system was the development of a suitable WFS as mentioned above.

Early solar AO technology experiments were carried out on the DST of the NSO, including the first solar AO experiment led by Hardy from 1979 to 1980 [169], the first solar AO system based on correlation SHWFS [170], etc. The successful application of correlating SHWFS makes the solar AO becoming a standard device of the large aperture ground-based solar telescope. The following Table 7 shows the solar AO systems that have been used and are being used.

The Gregor telescope, developed by KIS in Germany, is the largest coaxial open solar telescope in Europe. The effective aperture of the primary mirror is 1.5m. The telescope successfully made its first light in 2011 [171]. In the design stage of Gregor, the high-order solar AO system and MCAO system are fully considered as important components. At first, the Gregor solar AO system adopted the low-order correction mode. By correcting about the first 60 Zernike mode aberrations, and operating at 100Hz of closed-loop bandwidth, the system can only obtain the resolution near the diffraction-limited when the seeing is better than 0.6" [172]. In 2012, Gregor upgraded the system to a high-order AO system(GAOS256) with 256 units (the correlation SHWFS has 156 subapertures) [173]. Then the system can obtain diffraction

Table 7 The solar AO systems that have been used and are being used

Telescope/AO system	NO. subapertures	Number of actuators	Sampling frequency	Hardware architecture	First light
76cm DST/Lockheed	19	57	2kHz	Analog Circuits	1986
76cm DST/LOAO	24	97	1.6kHz	24 DSPs	1998
48cm SVST	19	19	955Hz	566MHz Alpha	1999
76cm DST/HOAO	76	97	2.5kHz	40 DSPs	2002
70cm VTT/KAOS	36	35	955Hz	8×900MHz Sun	2002
1.5m McMath-Pierce	120~200	37	955Hz	1GHz Pentium III	2002
97cm SST	37	37	955Hz	1.4GHz Athlon	2003
65cm BBSO/HOAO	76	97	2.5kHz	40 DSPs	2004
1.6m NST/HOAO	76	97	2.5kHz	40 DSPs	2010
1.6m NST/HOAO	308	349	2kHz	DSP clusters	2013
1.5m GREGOR/HOAO	156	256	2kHz	Multiple-CPU SMP	2012
1m NVST LOAO	30	37	2.1kHz	DSP and FPGA	2013
1m NVST HOAO	102	151	3.4kHz	DSP and FPGA	2015
1.8m CLST GLAO/HOAO	48/396	451	1.9kHz	Hybrid FPGA and CPU	2019
4m DKIST/HOAO	1457	1600	1.97	Hybrid FPGA and CPU	2019

-limited resolution when the seeing is better than 1.2", and can correct the first 170 Zernike aberrations at most. In November 2013, the Gregor telescope successfully obtained the closed-loop experimental results of solar observation [174]. From 2018 to 2020, the optical system (secondary mirror and relay optical system connected with AO), machinery and control system of Gregor telescope were further upgraded [175], and the imaging quality of AO was significantly improved, as shown in Fig. 23.

The 1.6m solar telescope of the BBSO GST (NST previously) has successively installed three sets of AO systems, AO76 [176], AO308 [168] and MCAO test system "Clear" [118]. During the initial GST phase, the AO system AO76 on the original 65 cm aperture solar telescope was installed and used. However, due to the limited correction ability, AO76 can only realize diffraction-limited observation in the near-infrared band and can not give full performance of GST's large aperture high-resolution observation. Subsequently, the team of BBSO cooperated with the NSO to carry out higher-order solar AO technology research and system development. At present, BBSO has successfully developed a high-order solar AO system AO308 with 357 units DM, which was put into operation in May 2013. The observations of the high-order solar AO system AO308 at BBSO was shown at Fig. 24 below (http://bbso.njit.edu/stuff/BBSO_AO-308_Poster.pdf).

The American 4m Daniel K. Inouye Solar Telescope (DKIST) is currently the world's largest solar telescope. It is finally equipped with 1600 units solar AO system, and the number of DM units is nearly 22% more than the original plan of 1313 actuators. The DM is developed by Northrop Grumman AOA xinetics, and the correction frequency can reach 2KHz. The correlation SHWFS has 1457 subapertures. The AO system can correct up to 1400 order KL modes [177]. In December 2019, DKIST was completed and launched its first light. Its AO system, as the first light instrument, successfully realized the closed loop by using the granulations of the solar photosphere as the wavefront detection beacon under the condition of Fried's parameter of 6cm ~ 7cm, and obtained

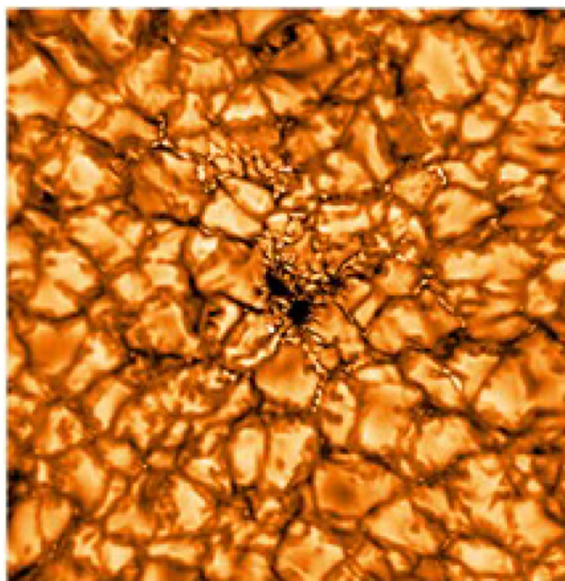


Fig. 23 The high resolution imaging results at solar photosphere after AO correction and speckle reconstruction obtained by Gregor telescope(2020.7) (<https://phys.org/news/2020-09-solar-teles-cope-gregor-unveils-magnetic.html>)

the high-resolution imaging results of the solar atmospheric photosphere quiet area which was shown at Fig. 25.

Solar AO technology in China started late but developed rapidly. China began to engage in the development of low-order tilt correction AO system in 1998 [178, 179]. Subsequently, through a series of technological breakthroughs and experience accumulation, many sets of AO systems were developed and equipped for the 26cm aperture solar fine structure telescope [180] and 1m NVST of Yunnan Observatory. Among them, the detection frequency of the WFS of the 37 units solar AO system can reach 2100Hz [181], the tracking accuracy after closed-loop is about 0.04"(RMS), and the error suppression bandwidth is about 110Hz. Due to the limitation of the number of wavefront corrector, the 37 units low-order solar AO system works under the condition of moderate seeing, and obtains the correction effect close to the diffraction-limited for the near-infrared band, but the performance is insufficient in the visible band. As a result, the solar high resolution imaging team of IOE, CAS successively solved the technical problems of solar AO system, such as high space and time bandwidth requirements, high

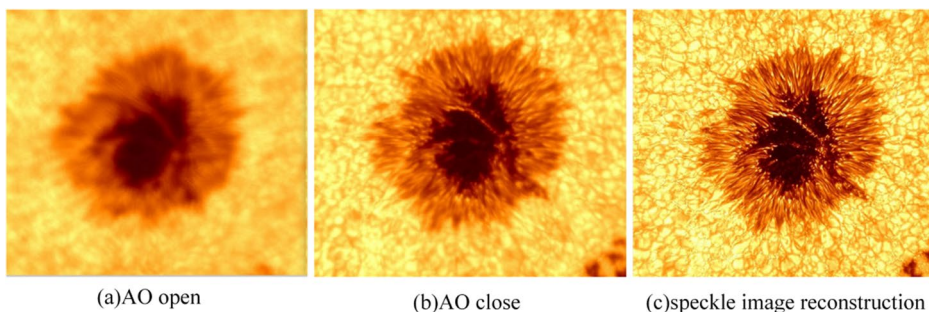


Fig. 24 The observations of the high-order solar AO system AO308 at BBSO

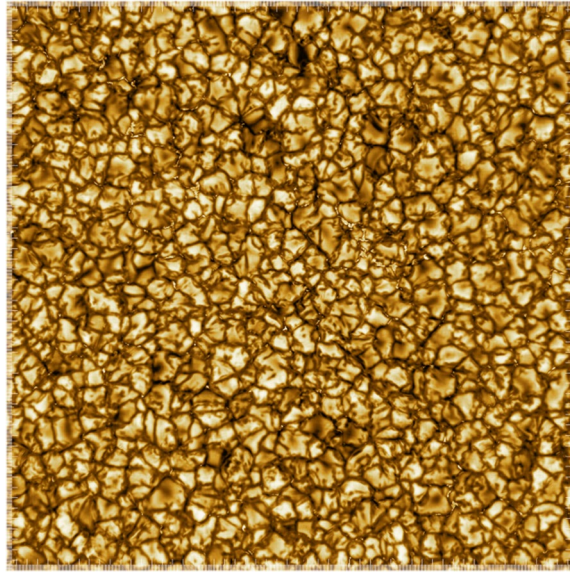


Fig. 25 The high-resolution imaging results of the quiet area obtained by 4m DKIST [177]

frame rate wavefront detection, high-speed wavefront real-time processing and control. By carrying out research on high-order solar AO technology, they eventually developed 151 units solar AO system with wavefront detection frame rate of 3500Hz around 2015 [182]. The results were shown at Fig. 26. In July 2015, the system was equipped at NVST and put into observation to obtain high resolution sunspots and granulations. Parallel to this, a number of major technical studies and test system developments have been made in relation to the next generation wide field AO technology. In 2016, the GLAO system was efficiently built [132], followed by the completion of MCAO system in early 2017 [133]. In December 2019, the 451 units high-order solar AO system integrated on the 1.8m solar telescope CLST successfully get its first light [183], as shown in Fig. 27. In April 2020, the high-order SHWFS, composed of 396 subapertures and a 451-element DM, was used to correct the atmospheric wavefront aberration and obtain the near diffraction-limited observation of the solar photosphere and chromosphere.

The future of AO in astronomy

The next-generation 30m class optical/infrared telescopes, along with some 4m class solar telescopes currently under construction, are being designed to employ AO systems.

The GMT is a 25m optical/infrared extremely large telescope which will start science operation in mid-2023. To simplify the overall optical control challenge and provide more pathways for realizing the exquisite imaging potential of the telescope, the GMT incorporates a seven-segment Gregorian DSM to implement three modes of AO operation: NGS AO, laser-tomography AO, and GLAO. The DSM will be used for all operating modes of AO on the GMT, as well as for open loop operation when installed [184]. Each DSM segment will have 672 electromagnetic actuators supporting a 2 mm thick face sheet, which provides the deformable surface for controlling the AO wavefront. The full DSM comprises seven segments, for a total of 4,704 actuators.

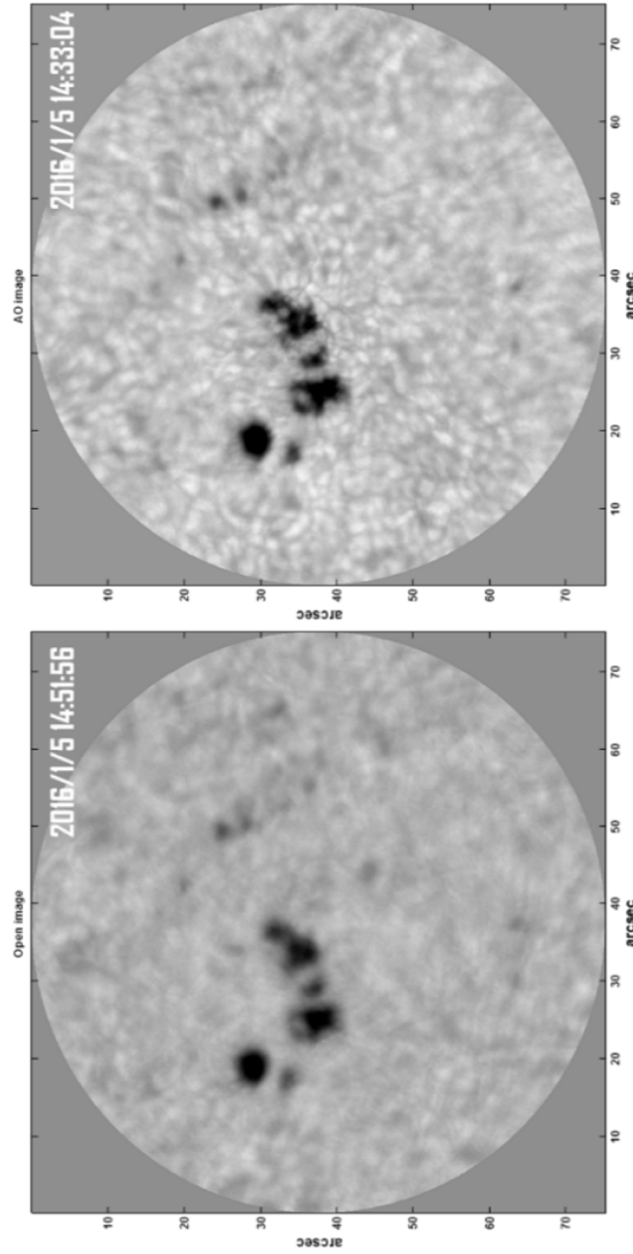


Fig. 26 Short exposure images of sunspot with AO off (left) and the 151 unit high-order AO system (right)(705.7nm@0.6nm)

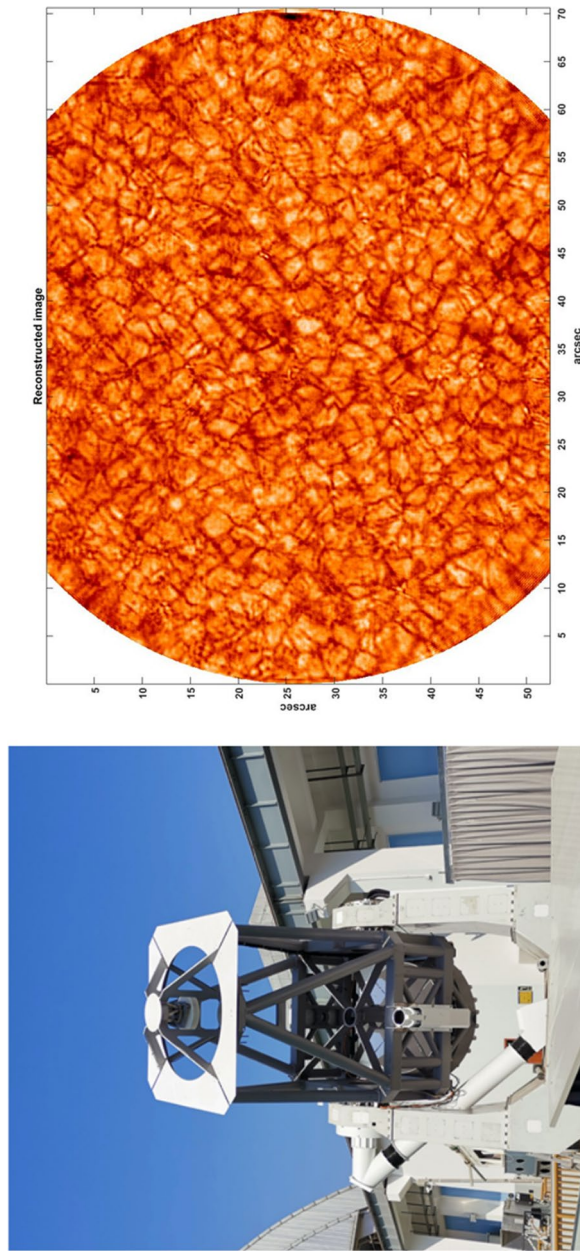


Fig. 27 High resolution imaging results of 451 units solar AO system for 1.8m solar telescope CLST (combined with speckle reconstruction)

GLAO: The wavefront aberration will be detected by using multiple wavefront sensors and compensated for by the DSM, this can improve natural seeing images over a FOV comparable to the GS constellation size. While providing some improvement in the visible band imaging, GLAO correction is expected to be particularly useful at observation wavelengths longer than $1\ \mu\text{m}$.

NGS AO: This mode uses a single bright star to determine image distortions and derive corrections needed to achieve diffraction-limited imaging. It is capable of producing high-quality images at wavelengths from the visible to the mid-infrared over a FOV of $20''$ - $30''$ in diameter.

Laser Tomography AO: This observing mode uses a $\sim 1'$ diameter constellation consisting of 6 LGSs to tomographically reconstruct the high-order components of the atmospheric wavefront aberrations in the direction of a central science target. Additionally, one faint NGS is used to measure tip-tilt, focus, segment piston, and dynamic calibration terms. The DSM will then compensate for the wavefront aberration, providing diffraction-limited imaging at 0.9 - $2.5\ \mu\text{m}$ wavelength over a FOV limited by atmospheric isoplanatism.

The first light instruments for the Thirty Meter Telescope (TMT) are the Infrared Imager and Spectrograph (IRIS) and the Infrared Multi-Slit Spectrograph (IRMS). Both instruments will take advantage of the Sodium LGS MCAO system named the Narrow-Field Infrared AO System (NFIRAOS) to achieve high spatial resolution. One particular feature of NFIRAOS is that it will be cooled to -30° to minimize thermal emissivity from the optics, which can affect the quality of observations [185]. NFIRAOS is supported on a Nasmyth platform of TMT and will provide near-diffraction-limited performance over a FOV ranging from $10''$ - $30''$. NFIRAOS comprises six LGSs wavefront sensors, one high-order NGS WFS for observations without LGS, and a truth WFS (TWFS). It also features two DMs, one of which is mounted on a tip-tilt stage. Additionally, NFIRAOS contains a source simulator (for natural objects and laser beacons), a phase screen and all associated entrance windows, beam splitters, fore-optics, opto-mechanical devices, cooling, electronics and computing systems. Furthermore, It includes test equipment, consisting of a high-resolution WFS, acquisition camera, and miscellaneous fixtures.

MAORY is a Sodium LGS MCAO system that feeds the MICADO (Multi-AO Imaging Camera for Deep Observations) for ELT [186]. The system is currently in phase B, and provides a uniform and high quality SR over a FOV of $60''$ for wavelengths between 0.8 - $2.4\ \mu\text{m}$. The turbulence is measured using a configuration of 6 Sodium LGSs (which will be upgraded to 8 sodium LGSs located at the edge of a circle with a diameter of $45''$) and 3 NGSs (brighter than 21 magnitude), allowing for sky coverage of the AO system up to 50%. The system will use 3 DMs for compensation. One of them is the secondary mirror of the telescope, DM M4, which has 5000 actuators conjugated at several hundred meters above the pupil of the telescope. In addition to this, there are two post-focal DMs conjugated at 4km and 12.7km , respectively. Each post-focal DM contains at least 1500 actuators.

In solar observation, DKIST is going to be upgraded with MCAO, including the WFS system, the real-time control system and the DM systems [187]. The WFS system consists of nine correlating SH-WFSs, each with approximately a $10''\times 10''$ FOV and a frame rate of around 2000 fps. In MCAO mode, the WFS system has 41 subapertures across

the pupil (1313 total), and the FOV is adjustable from about 30"×30" to 60"×60" depending on the turbulence profiles. The real-time control system is a cluster of ten x86-64 servers, including nine WFS nodes and one controller node. All servers are interconnected with Infiniband HDR. Each sensor node is connected to one WFS camera and extracts the slope of each subaperture. The controller node adds up the results of all WFS nodes and sends commands to the DM. The real-time control system can operate at 2000 fps in MCAO mode. The DM systems include three DMs conjugated to 0, 4 and 11.2 kilometers. The number of the DM actuators conjugated at 0km and 4km are 1600 and 1600, respectively. The actuator number of rest DM is still to be determined.

The European Solar Telescope (EST) [188] is currently under development and is expected to be completed by 2028. With 4m aperture, EST incorporates a powerful AO system, including GLAO and MCAO [189] to achieve the desired high spatial resolution. To correct for turbulence over a wide range of observing elevations, from the zenith to nearly the horizon, a configuration of 4 high-altitude DMs is used. In GLAO mode, the ground layer DM and a high order correlating SHWFS are employed. Two WFSs are used, each with ~2000 subapertures. The subapertures have sizes of 8cm and 30cm, with a sensing field size of 10"×10". The artificial neural networks (ANNs), which have been used at AO system recently, is also considered to sense the wavefront error in the MCAO test bed. To achieve the required corrected FOV of 1'×1', the stratification of turbulence (Cn²) with height above the telescope site is used to inform the MCAO optical design (in particular the number and size of the conjugate high altitude DMs). The actuators spacings of the five DMs are 8cm, 8cm, 30cm, 30cm, 30cm, for a total of approximately ~4000 actuators. In addition, to substantially improve the optical quality and the photon flux in the science focus, the optical design has been updated to incorporate a DSM. This new concept simplifies the optical design, reducing the number of optical surfaces before the instrument suite, and results in an increase in the photon flux by a factor of approximately 2, depending on the wavelength.

Recent work by Guo et al. has reviewed the progress of AO techniques based on machine learning. The wavefront sensing, wavefront reconstruction and post-processing will be all greatly improved by the artificial intelligent (AI) algorithms [9]. For example, in wavefront sensing, the phase retrieval speed from phase diversity images, or even single modulated image, is substantially accelerated [190]. For SHWFS, higher spatial resolution for the aberration measurement is also achieved by using the machine learning to extract more information from the SHWFS's images [191]. In wavefront control, machine learning algorithms such as long short-term memory neural networks have enabled the prediction of future wavefront based on historical data, which is especially important for extreme AO [192]. In post-processing, real-time imaging post-processing may also be achieved through the use of pre-trained neural networks [175]. Besides all of the advancements mentioned above on single component of AO, the whole system may be further reformed by artificial intelligence. For instance, the fully automatic operation of AO system for high efficiency and rapid response. The self-perception and calibration of the AO system's misalignment and faults. In summary, the development of AI has the potential to significantly improve the performance and capabilities of AO systems.

Conclusions

During the past 50 years of rapid development, AO systems have been widely used in the field of astronomical observation. Almost all large aperture optical telescopes for high resolution observation are equipped with AO systems to correct the wavefront distortions caused by atmospheric turbulence and the static aberrations of the telescopes. To meet new application requirements, AO technology is continuously innovating at wavefront detection, wavefront correction and wavefront controlling. New technologies and system architectures, such as LGS AO, DSM, ExAO and wide field AO, etc., are rapidly advancing to greatly improve telescope performance. Nowadays, the excellent performance of AO systems make them an indispensable part of the night-time astronomy and solar telescopes under construction and in the future. It is believed that observation results obtained from the large aperture optical telescopes equipped with advanced AO systems will expand mankind's vision, produce subversive scientific research achievements, and promote the further development and application of AO technology.

Abbreviations

AO	Adaptive Optics
ESO	European Southern Observatory
NOAO	National Optical Observatories
FOV	Field of view
MCAO	Multi-layer Conjugation Adaptive Optics
MOAO	Multi-object Adaptive Optics
GLAO	Ground Layer Adaptive Optics
GMT	Giant Magellan Telescope
TMT	Thirty-Meter Telescope
ELT	European Extremely Large Telescope
LGS	Laser Guide Star
DSM	Deformable Secondary Mirror
VCDSM	Voice-coil DSM
ExAO	Extreme Adaptive Optics
DM	Deformable Mirror
WFS	Wavefront Sensor
SHWFS	Shack Hartmann wavefront sensor
NTT	New Technology Telescope
ASM	Adaptive Secondary Mirror
IOE	Institute of optics and electronics
CAS	Chinese Academy of sciences
NSO	National Solar Observatory
BBSO	Big Bear Solar Observatory
SR	Strehl ratio
MR	Magnitude range
vis	Visible band
NIR	Near infrared band
DKIST	Daniel K. Inouye Solar Telescope
GS	Guide stars
NGS	Natural guide stars
VC	Voice-coil
VCDSM	Voice-coil DSM
PSF	Point spread function
AI	Artificial intelligent

Acknowledgements

MS. Tang Yu, MS. Fu Xiaofang, Dr. Huang Jian, Dr. Deng Keran and Ke Zibo, Yan Nanfei from Institute of Optics and Electronics, Chinese Academy of Sciences, are acknowledged for their contribution.

Authors' contributions

C.H.R. and L.B.Z. were major contributors in writing the manuscript. Y.M.G. prepared the part of Deformable Secondary Mirror. L.Q.Z. prepared the part of wide field AO technology. M.L. and K.W. prepared the part of LGS AO. All authors revised the paper and approved the final manuscript.

Authors' information

Changhui Rao: Corresponding author (chrao@ioe.ac.cn). The Key Laboratory on Adaptive Optics, Chinese Academy of Sciences, Chengdu, China; Institute of Optics and Electronics, Chinese Academy of Sciences, Chengdu, China; The University

of Chinese Academy of Sciences, Beijing, China. Libo Zhong: The Key Laboratory on Adaptive Optics, Chinese Academy of Sciences, Chengdu, China; Institute of Optics and Electronics, Chinese Academy of Sciences, Chengdu, China. Youming Guo: The Key Laboratory on Adaptive Optics, Chinese Academy of Sciences, Chengdu, China; Institute of Optics and Electronics, Chinese Academy of Sciences, Chengdu, China. Min Li: The Key Laboratory on Adaptive Optics, Chinese Academy of Sciences, Chengdu, China; Institute of Optics and Electronics, Chinese Academy of Sciences, Chengdu, China. Lan-qiang Zhang: The Key Laboratory on Adaptive Optics, Chinese Academy of Sciences, Chengdu, China; Institute of Optics and Electronics, Chinese Academy of Sciences, Chengdu, China. Kai Wei: The Key Laboratory on Adaptive Optics, Chinese Academy of Sciences, Chengdu, China; Institute of Optics and Electronics, Chinese Academy of Sciences, Chengdu, China; The University of Chinese Academy of Sciences, Beijing, China.

Funding

This work was funded by the National Natural Science Foundation of China (11727805, 11733005, 12173041, 12103057) and Frontier Research Fund of Institute of Optics and Electronics, Chinese Academy of Sciences C21K002.

Availability of data and materials

Data sharing is not applicable to this article as no datasets were generated or analysed during the current study.

Declarations

Ethics approval and consent to participate

Not applicable.

Consent for publication

Not applicable.

Competing interests

The authors declare that they have no competing interests.

Received: 12 May 2023 Revised: 15 December 2023 Accepted: 16 January 2024

Published online: 01 May 2024

References

- Babcock HW. The possibility of compensating astronomical seeing. *Publ Astron Soc Pac.* 1953;65:229. <https://doi.org/10.1086/126606>.
- Hardy JW, Lefebvre JE, Koliopoulos CL. Real-time atmospheric compensation. *J Opt Soc Am.* 1977;67(3):360–9. <https://doi.org/10.1364/JOSA.67.000360>.
- Kern P, Merkle F, Gaffard JP, Rousset G, Fontanella JC, Lena P. Prototype Of An Adaptive Optical System For Astronomical Observation. *Proc. SPIE 0860, Real-Time Image Processing: Concepts and Technologies.* 1988. <https://doi.org/10.1117/12.943379>.
- Beckers JM. Increasing the size of the isoplanatic patch with multiconjugate adaptive optics. *Very Large Telescopes and their Instrumentation, ESO Conference and Workshop Proceedings, Proceedings of a ESO Conference on Very Large Telescopes and their Instrumentation, held in Garching, March 21–24, 1988.* Garching: European Southern Observatory (ESO); 1988. p. 693. edited by Marie-Helene Ulrich.
- Lamb M, Venn K, Andersen D, Oya S, Shetrone M, Fattahi A, Howes L, Asplund M, Lardiére O, Akiyama M, et al. Using the multi-object adaptive optics demonstrator raven to observe metal-poor stars in and towards the Galactic Centre. *Mon Not R Astron Soc.* 2016;2865
- Rigaut F. Ground conjugate wide field adaptive optics for the elts. *Beyond conventional adaptive optics: a conference devoted to the development of adaptive optics for extremely large telescopes. Proceedings of the Topical Meeting held May 7–10, 2001, Venice, Italy.* Edited by E. Vernet, R. Ragazzoni, S. Esposito, and N. Hubin. Garching, Germany: European Southern Observatory; 2002. p. 11. *ESO Conference and Workshop Proceedings, Vol. 58, ISBN 3923524617.*
- Wizinowich P. Adaptive optics in astronomy. *Contemp Phys.* 2015;56(4):432–50. <https://doi.org/10.1080/00107514.2015.1041765>.
- Hippler S. Adaptive optics for extremely large telescopes. *J Astron Instrum.* 2019;08(02):1950001. <https://doi.org/10.1142/S2251171719500016>.
- Guo Y, Zhong L, Min L, Wang J, Wu Y, Chen K, Wei K, Rao C. Adaptive optics based on machine learning: a review. *Opto-Electron Adv.* 2022;5(20082):200082–120008220. <https://doi.org/10.29026/oea.2022.200082>.
- d'Orgeville C, Fetzer GJ. Four generations of sodium guide star lasers for adaptive optics in astronomy and space situational awareness. *Proc. SPIE 9909, Adaptive Optics Systems V, 99090R.* 2016. <https://doi.org/10.1117/12.2234298>.
- Wizinowich P. Adaptive optics in astronomy. *Contemp Phys.* 2015;56:1–19. <https://doi.org/10.1080/00107514.2015.1041765>.
- Matijevich R, Johansson E, Johnson L, et al. Bringing Perfect Vision to the Daniel K. Inoué Solar Telescope. *American Astronomical Society Meeting Abstracts# 227.* 227: 146.21, 2016.
- Stroebele S, Vernet E, Brinkmann M, Jakob G, Lilley P, Casali M, et al. Deformable mirrors development program at ESO. *Proc. SPIE 9909, Adaptive Optics Systems V, 99090O.* 2016. <https://doi.org/10.1117/12.2232536>.
- Huang L, Zheng Y, Guo Y, Zhang L, Sun C, Wang X. 21.2 kw, 1.94 times diffraction-limit quasi-continuous-wave laser based on a multi-stage, power-scalable and adaptive optics controlled yb: yag master-oscillator-power-amplifier system. *Chin Opt Lett.* 2020;18(11):061402.

15. Laslandes M. Towards the spatialization of ALPA dms. Proceedings of the SPIE, Volume 11852, id. 118524J 11 pp. 2021.
16. Samarkin V, Alexandrov A, Borsoni G, Jitsuno T, Romanov P, Rukosuev A, Kudryashov A. Wide aperture piezoceramic deformable mirrors for aberration correction in high-power lasers. *High Power Laser Sci Eng.* 2016;4:22–8.
17. Zhang Y, Yuan Y, Zhou H, Liu H, Fang J, Zhang A, Xian H. Lightweight unimorph mirror using an optical replication method. *Opt Eng.* 2019;58(8):085101. <https://doi.org/10.1117/1.OE.58.8.085101>.
18. Chen J, Ma J, Zuo H, Yuan X, Li B, Chu J. Woofer–tweeter deformable mirror driven by combined actuators with a piezoelectric unimorph and stack for astronomical application. *Appl Opt.* 2019;58(9):2358–65. <https://doi.org/10.1364/AO.58.002358>.
19. Biasi R, Manetti M, Andrighettoni M, Angerer G, Pescoller D, Patauner C, et al. E-ELT M4 adaptive unit final design and construction: a progress report. Proc. SPIE 9909, Adaptive Optics Systems V, 99097Y. 2016. <https://doi.org/10.1117/12.2234735>.
20. Kuiper S, Doelman N, Overtoom T, Nieuwkoop E, Russchenberg T, van Riel M, et al. Electromagnetic deformable mirror for space applications. Proc. SPIE 10562, International Conference on Space Optics — ICSSO 2016, 1056230. 2017. <https://doi.org/10.1117/12.2296161>.
21. Zuo H, Li G, Pan C. Non-contact displacement measure method based on eddy current sensors in the large aperture adaptive mirror system. Proc. SPIE 10703, Adaptive Optics Systems VI, 107037B. 2018. <https://doi.org/10.1117/12.2312340>.
22. Hartley R, Kartz MW, Behrendt WC, Hines A, Pollock G, Bliss ES, et al. Wavefront correction for static and dynamic aberrations to within 1 second of the system shot in the NIF Beamlet demonstration facility. Proc. SPIE 3047, Solid State Lasers for Application to Inertial Confinement Fusion: Second Annual International Conference. 1997. <https://doi.org/10.1117/12.294315>.
23. Munro J, Travouillon T, Lingham M. Fast pixel difference algorithm for determining piston step between optical mirror segments. Proceedings of the SPIE, Volume 11448, id. 114486H 11 pp. 2020. 41.
24. Cheetham A, Cvetojevic N, Norris B, Sivaramakrishnan A, Tuthill P. Fizeau interferometric cophasing of segmented mirrors: experimental validation. *Opt Express.* 2014;22(11):12924–34.
25. Wilburn B, Joshi N, Vaish V, Talvala E-V, Antunez E, Barth A, Adams A, Horowitz M, Levoy M. High performance imaging using large camera arrays. *ACM Trans Graph.* 2005;24(3):765–76. <https://doi.org/10.1145/1073204.1073259>.
26. Ng R, Levoy M, Brédif M, Duval G, Horowitz M, Hanrahan P. Light field photography with a hand-held plenoptic camera. Tech Rep CTSR 2005-02. 2005;CTSR.
27. Veeraraghavan A, Raskar R, Agrawal A, Mohan A, Tumblin J. Dappled photography: mask enhanced cameras for heterodyned light fields and coded aperture refocusing. *ACM Trans Graph.* 2007;26(3):69. <https://doi.org/10.1145/1276377.1276463>.
28. Marwah K, Wetzstein G, Bando Y, Raskar R. Compressive light field photography using overcomplete dictionaries and optimized projections. *ACM Trans. Graph.* 2013;32(4). <https://doi.org/10.1145/2461912.2461914>
29. Lukin V. Adaptive optical imaging in the atmosphere. *USP FIZ Nauk.* 2006;176. <https://doi.org/10.3367/JFNr.0176.200609j.1000>
30. Bian Q, Bo Y, Zuo J-W, Li M, Feng L, Wei K, Wang R-T, Li H-Y, Peng Q-J, Xu Z-Y. First implementation of pulsed sodium guidestars constellation for large-aperture multi-conjugate adaptive optics telescopes. *Publ Astron Soc Pac.* 2022;134(1037):074502. <https://doi.org/10.1088/1538-3873/ac7c8e>.
31. Neichel B, Lu JR, Rigaut F, Ammons SM, Carrasco ER, Lassalle E. Astrometric performance of the gemini multi-conjugate adaptive optics system in crowded fields. *Mon Not R Astron Soc.* 2014;445(1):500–14. <https://doi.org/10.1093/mnras/stu1766>.
32. Benedict J, Rittig, Breckinridge JB, Fried DL. Introduction: Atmospheric-compensation technology. *J Opt Soc Am A.* 1994;11(1):257–262. <https://doi.org/10.1364/JOSAA.11.000257>
33. Foy R, Labeyrie A. Feasibility of adaptive telescope with laser probe. *Astron Astrophys.* 1985;152(2):29–31.
34. Fugate RQ, Ellerbroek BL, Higgins CH, Jelonek MP, Lange WJ, Slavin AC, Wild WJ, Winker DM, Wynia JM, Spinhirne JM, Boeke BR, Ruane RE, Moroney JF, Oliker MD, Swindle DW, Cleis RA. Two generations of laser-guide-star adaptive-optics experiments at the starfire optical range. *J Opt Soc Am A.* 1994;11(1):310–24. <https://doi.org/10.1364/JOSAA.11.000310>.
35. Thompson LA, Teare SW. Rayleigh laser guide star systems: application to the university of illinois seeing improvement system. *Publ Astron Soc Pac.* 2002;114(799):1029.
36. Thompson LA, Teare SW, Xiong Y-H, Castle RM, Chakraborty A, Gruendl RA, Leach RW. Unisis: Laser guide star and natural guide star adaptive optics system. *Publ Astron Soc Pac.* 2009;121(879):498.
37. Happer W, MacDonald GJ, Max CE, Dyson FJ. Atmospheric-turbulence compensation by resonant optical back-scattering from the sodium layer in the upper atmosphere. *J Opt Soc Am A.* 1994;11(1):263–76. <https://doi.org/10.1364/JOSAA.11.000263>.
38. Max CE, Olivier SS, Friedman HW, An J, Avicola K, Beeman BV, Bissinger HD, Brase JM, Erbert GV, Gavel DT, Kanz K, Liu MC, Macintosh B, Neeb KP, Patience J, Waltjen KE. Image improvement from a sodium-layer laser guide star adaptive optics system. *Science.* 1997;277(5332):1649–52. <https://doi.org/10.1126/science.277.5332.1649> <https://www.science.org/doi/pdf/10.1126/science.277.5332.1649>
39. Wizinowich PL, Le Mignant D, Bouchez AH, Campbell RD, Chin JC, Contos AR, van Dam MA, Hartman SK, Johansson EM, Lafon RE, et al. The WM Keck Observatory laser guide star adaptive optics system: overview. *Publ Astron Soc Pac.* 2006;118(840):297. <https://iopscience.iop.org/article/10.1086/499290/meta>.
40. van Dam MA, Bouchez AH, Le Mignant D, Johansson EM, Wizinowich PL, Campbell RD, Chin JC, Hartman SK, Lafon RE, Stomski PJ, et al. The WM Keck Observatory laser guide star adaptive optics system: performance characterization. *Publ Astron Soc Pac.* 2006;118(840):310.
41. Ramey E, Lu JR, Yin R, Robinson S, Wizinowich P, Ragland S, Lyke J, Jia S, Sakai S, Gautam A, et al. Analyzing long-term performance of the keck-ii adaptive optics system. In: Adaptive Optics Systems VII, vol. 11448, 2020. p. 1010–1026.

42. Chin JCY, Wizinowich P, Wetherell E, Cetre S, Ragland S, Campbell R, et al. Laser guide star facility developments at W. M. Keck Observatory. *Proc. SPIE* 9148, Adaptive Optics Systems IV, 914808. 2014. <https://doi.org/10.1117/12.2057449>.
43. Chin JCY, Stalcup T, Wizinowich P, Pantelev S, Neyman C, Tsubota K, et al. Keck I laser guide star AO system integration. *Proc. SPIE* 7736, Adaptive Optics Systems II, 77361V. 2010. <https://doi.org/10.1117/12.857598>.
44. Wizinowich P, Dekany R, Gavel D, Max C, Adkins S, Bauman B, et al. W. M. Keck Observatory's next-generation adaptive optics facility. *Proc. SPIE* 7015, Adaptive Optics Systems, 701511. 2008. <https://doi.org/10.1117/12.790154>.
45. Chen GC-F, Fassnacht CD, Suyu SH, Rusu CE, Chan JHH, Wong KC, et al. A sharp view of h0licow: H0 from three time-delay gravitational lens systems with adaptive optics imaging. *Mon Not R Astron Soc.* 2019;490(2):1743–1773.
46. Guyon O, Hayano Y, Tamura M, Kudo T, Oya S, Minowa Y, et al. Adaptive optics at the Subaru telescope: current capabilities and development. In: Adaptive Optics Systems IV, vol. 9148, 2014. p. 609–618. <https://doi.org/10.1117/12.2057273>.
47. Calia DB, Allaert E, Alvarez JL, Hauck CA, Avila G, Bendek E, et al. First light of the ESO laser guide star facility. In: Ellerbroek BL, Calia DB (eds.) *Advances in Adaptive Optics II*, vol. 6272, 2006. p. 50–60. <https://doi.org/10.1117/12.674484>.
48. Norton AP, Gavel DT, Helmbrecht M, Kempf C, Gates E, Chloros K, et al. Laser guidestar uplink correction using a MEMS deformable mirror: on-sky test results and implications for future AO systems. *Proc. SPIE* 9148, Adaptive Optics Systems IV, 91481C. 2014. <https://doi.org/10.1117/12.2055564>.
49. Paufigue J, Bruton A, Glindemann A, Jost A, Kolb J, Jochum L, Le Louarn M, Kiekebusch M, Hubin N, Madec P-Y, Conzelmann R, Siebenmorgen R, Donaldson R, Arsenault R, Tordo S. GRAAL: a seeing enhancer for the NIR wide-field imager Hawk-I. In: Ellerbroek BL, Hart M, Hubin N, Wizinowich PL (eds.) *Adaptive Optics Systems II. Society of Photo-Optical Instrumentation Engineers (SPIE) Conference Series*, vol. 7736, 2010. p. 77361. <https://doi.org/10.1117/12.858261>
50. Paufigue J, Argomedo J, Arsenault R, Conzelmann R, Donaldson R, Hubin N, Jochum L, Jost A, Kiekebusch M, Kolb J, Kuntschner H, Louarn M, Madec P-Y, Siebenmorgen R, Tordo S. Status of the graal system development: Very wide-field correction with 4 laser guide-stars. *Proc SPIE Int Soc Opt Eng.* 2012;8447:38. <https://doi.org/10.1117/12.927265>.
51. Fedrigo E, Bourtembourg R, Donaldson R, Soenke C, Valles MS, Zampieri S. SPARTA for the VLT: status and plans. *Proc. SPIE* 7736, Adaptive Optics Systems II, 77362I. 2010. <https://doi.org/10.1117/12.857084>.
52. Girard JH, de Boer J, Haffert S, Zeidler P, Bohn A, van Holstein RG, Snellen I, Brinchmann J, Keller C, Bacon R, Bae J. Original use of MUSE's laser tomography adaptive optics to directly image young accreting exoplanets, 2020. <http://arxiv.org/abs/2003.02145>
53. Herriot G, Morris S, Roberts SC, Fletcher JM, Saddlemyer LK, Singh G, Veran J-P, Richardson EH. Innovations in Gemini adaptive optics system design. In: Bonaccini D, Tyson RK, editors. *Adaptive Optical System Technologies*, vol. 3353, 1998. p. 488–499. <https://doi.org/10.1117/12.321684>.
54. Chun M, D'Orgeville C, Ellerbroek L, Graves J, Northcott M, Rigaut F. Curvature-based laser guide star adaptive optics system for gemini south. *Proc SPIE*, 2000. p. 142–148. <https://doi.org/10.1117/12.390399>
55. Hackenberg WKP, Bonaccini D, Werner D. Fiber Raman laser development for multiple sodium laser guide star adaptive optics. *Proc. SPIE* 4839, Adaptive Optical System Technologies II. 2003. <https://doi.org/10.1117/12.458930>.
56. James E, Boyer C, Buchroeder R, Ellerbroek B, Hunten M. Design considerations of the ao module for the gemini south multiconjugate adaptive optics system. *Proc SPIE Int Soc Opt Eng.* 2003. <https://doi.org/10.1117/12.457082>.
57. Neichel B, Rigaut F, Vidal F, van Dam M, Garrel V, Carrasco ER, Pessev P, Winge C, Boccas M, D'Orgeville C, Arriagada G, Serio A, Fesquet V, Rambold W, Luhrs J, Moreno C, Gausachs G, Galvez R, Montes V, Edwards M. Gemini multi-conjugate adaptive optics system review ii: Commissioning, operation and overall performance. *Mon Not R Astron Soc.* 2014;440. <https://doi.org/10.1093/mnras/stu403>
58. Ferrero LV, Günthardt G, García L, Gómez M, Kalari VM, Saldaño HP. High-resolution images of two wiggling stellar jets, mho 1502 and mho 2147, obtained with gsaoi+gems. *Astron Astrophys.* 2022;657:110. <https://doi.org/10.1051/0004-6361/202142421>.
59. Jin K, Wei K, Feng L, Bo Y, Zuo J, Li M, Fu H, Dai X, Bian Q, Yao J, Xu C, Wang Z, Peng Q, Xue X, Cheng X, Rao C, Xu Z, Zhang Y. Photon return on-sky test of pulsed sodium laser guide star with d_{2b} repumping. *Publ Astron Soc Pac.* 2015;127(954):749–56. <https://doi.org/10.1086/682672>.
60. Beckers JM. A proposal to the National Science Foundation, in the NOAO 8M Telescope Description Vol. II, by the Association for University Research in Astronomy. 1989.
61. Lloyd-Hart M. Thermal performance enhancement of adaptive optics by use of a deformable secondary mirror. *Publ Astron Soc Pac.* 2000;112(768):264.
62. Stroebele S, Arsenault R, Bacon R, Biasi R, Bonaccini-Calia D, Downing M, Conzelmann R, Delabre B, Donaldson R, Duchateau M, et al. The eso adaptive optics facility. In: *Advances in Adaptive Optics II*, vol. 6272. International Society for Optics and Photonics; 2006. p. 62720.
63. Myers RM. Recent progress and perspectives for GLAO and MOAO. *Proc. SPIE* 7736, Adaptive Optics Systems II, 773622. 2010. <https://doi.org/10.1117/12.856704>.
64. Lee J, Bigelow B, Walker D, Doel A, Bingham R. Why adaptive secondaries? *Publ Astron Soc Pac.* 2000;112(767):97.
65. Esposito S, Riccardi A, Pinna E, Puglisi A, Quirós-Pacheco F, Arcidiacono C, et al. Large Binocular Telescope Adaptive Optics System: new achievements and perspectives in adaptive optics. *Proc. SPIE* 8149, Astronomical Adaptive Optics Systems and Applications IV, 814902. 2011. <https://doi.org/10.1117/12.898641>.
66. Close LM, Gasho V, Kopon D, Hinz PM, Hoffmann WF, Uomoto A, et al. The Magellan Telescope adaptive secondary AO system. *Proc. SPIE* 7015, Adaptive Optics Systems, 70150Y. 2008. <https://doi.org/10.1117/12.789527>. 247.
67. Arsenault R, Biasi R, Gallieni D, Riccardi A, Lazzarini P, Hubin N, et al. A deformable secondary mirror for the VLT. *Proc. SPIE* 6272, *Advances in Adaptive Optics II*, 62720V. 2006. <https://doi.org/10.1117/12.672879>.

68. Biasi R, Veronese D, Andrighettoni M, Angerer G, Gallieni D, Mantegazza M, Tintori M, Lazzarini P, Manetti M, Johns M, et al. Gmt adaptive secondary design. In: *Adaptive Optics Systems II*, vol. 7736, International Society for Optics and Photonics; 2010. p. 77363.
69. Gallieni D, Tintori M, Mantegazza M, Anaclerio E, Crimella L, Acerboni M, Biasi R, Angerer G, Andrighettoni M, Merler A, et al. Voice-coil technology for the e-elt m4 adaptive unit. In: *1st AO4ELT conference-Adaptive Optics for Extremely Large Telescopes*. EDP Sciences; 2010. p. 06002.
70. Kuiper S, Jonker W, Maniscalco M, Priem H, Coolen C, Chun M, Baranec C, Lu J, Lai O. Adaptive Secondary Mirror development for the UH-88 telescope. In: *AO4ELT6*, Quebec, Canada; 2019. <https://hal.archives-ouvertes.fr/hal-02384381>
71. Guo Y, Zhang A, Fan X, Rao C, Wei L, Xian H, Wei K, Zhang X, Guan C, Li M, Zhou L, Jin K, Zhang J, Deng J, Zhou L, Chen H, Zhang X, Zhang Y. First on-sky demonstration of the piezoelectric adaptive secondary mirror. *Opt Lett*. 2016;41(24):5712–5. <https://doi.org/10.1364/ol.41.005712>.
72. Riccardi A, Brusa G, Salinari P, Gallieni D, Biasi R, Andrighettoni M, Martin HM. Adaptive secondary mirrors for the Large Binocular Telescope. *Proc. SPIE 4839, Adaptive Optical System Technologies II*, (7 February 2003). <https://doi.org/10.1117/12.458961>.
73. Close LM, Males JR, Kopon D, Gasho V, Follette KB, Hinz P, et al. First closed-loop visible AO test results for the advanced adaptive secondary AO system for the Magellan Telescope: MagAO's performance and status. In: *Adaptive Optics Systems III Article 84470X (Proceedings of SPIE - The International Society for Optical Engineering; Vol. 8447)*. 2012. <https://doi.org/10.1117/12.926545>.
74. Close LM, Males JR, Follette KB, Hinz P, Morzinski K, Wu Y-L, et al. Into the blue: AO science with MagAO in the visible. *Proc. SPIE 9148, Adaptive Optics Systems IV*, 91481M. 2014. <https://doi.org/10.1117/12.2057297>.
75. Guo Y, Zhang A, Fan X, Rao C, Wei L, Xian H, et al. First light of the deformable secondary mirror-based adaptive optics system on 1.8m telescope. *Proc. SPIE 9909, Adaptive Optics Systems V*, 99091D. 2016. <https://doi.org/10.1117/12.2231842>.
76. Guo YM, Chen KL, Zhou JH, Li ZD, Han WY, et al. High-resolution visible imaging with piezoelectric deformable secondary mirror: experimental results at the 1.8-m adaptive telescope. *Opto-Electron Adv*. 2023;6:230039.
77. Guyon O. Extreme adaptive optics. *Annu Rev Astron Astrophys*. 2018;56:315–55.
78. Angel JRP. Ground-based imaging of extrasolar planets using adaptive optics. *Nature*. 1994;368(6468):203–7.
79. Stahl SM, Sandler DG. Optimization and performance of adaptive optics for imaging extrasolar planets. *Astrophys J*. 1995;454(2):153.
80. Nakajima T. Planet detectability by an adaptive optics stellar coronagraph. *Astrophys J*. 1994;425:348–57.
81. Mayor M, Queloz D. A jupiter-mass companion to a solar-type star. *Nature*. 1995;378(6555):355–9.
82. Macintosh B, Graham JR, Ingraham P, Konopacky Q, Marois C, Perrin M, Poyneer L, Bauman B, Barman T, Burrows AS, et al. First light of the gemini planet imager. *Proc Natl Acad Sci*. 2014;111(35):12661–6.
83. Milli J, Mouillet D, Fusco T, Girard J, Masciadri E, Pena E, Sauvage J-F, Reyes C, Dohlen K, Beuzit J-L, et al. Performance of the extreme-ao instrument vlt/sphere and dependence on the atmospheric conditions. *arXiv preprint arXiv:1710.05417* (2017)
84. Meeker SR, Truong TN, Roberts JE, Shelton JC, Fregoso SF, Burruss RS, Dekany RG, Wallace JK, Baker JW, Heffner CM, Mawet D, Rykoski KM, Tesch JA, Vasisht G. Design and performance of the PALM-3000 3.5 kHz upgrade. In: Schreiber L, Schmidt D, Vernet E (eds) *Adaptive Optics Systems VII*, vol. 11448, 2020. p. 192–204. <https://doi.org/10.1117/12.2562931>.
85. Dekany R, Roberts J, Burruss R, Bouchez A, Truong T, Baranec C, Guiwits S, Hale D, Angione J, Trinh T, et al. Palm-3000: exoplanet adaptive optics for the 5 m hale telescope. *Astrophys J*. 2013;776(2):130.
86. Macintosh B, Graham J, Palmer D, Doyon R, Gavel D, Larkin J, et al. The Gemini Planet Imager. In: Ellerbroek BL, Calia DB (eds) *Advances in Adaptive Optics II*, vol. 6272, 2006. p. 177–188. <https://doi.org/10.1117/12.672430>.
87. Graham JR, Macintosh B, Doyon R, Gavel D, Larkin J, Levine M, Oppenheimer B, Palmer D, Saddlemyer L, Sivaramakrishnan A, et al. Ground-based direct detection of exoplanets with the gemini planet imager (GPI), 2007. *arXiv preprint arXiv:0704.1454*
88. Ruffio J-B, Macintosh B, Wang JJ, Pueyo L, Nielsen EL, De Rosa RJ, Czekala I, Marley MS, Arriaga P, Bailey VP, et al. Improving and assessing planet sensitivity of the gpi exoplanet survey with a forward model matched filter. *Astrophys J*. 2017;842(1):14.
89. Konopacky QM, Rameau J, Duchêne G, Filippazzo JC, Godfrey PAG, Marois C, et al. DISCOVERY OF A SUBSTELLAR COMPANION TO THE NEARBY DEBRIS DISK HOST HR 2562. *Astrophys J*. 2016;829(1):4. <https://doi.org/10.3847/2041-8205/829/1/4>.
90. Oppenheimer BR, Beichman C, Brenner D, Burruss R, Cady E, Crepp J, et al. Project 1640: the world's first ExAO coronagraphic hyperspectral imager for comparative planetary science. In: Ellerbroek BL, Marchetti E, Véran J-P (eds) *Adaptive Optics Systems III*, vol. 8447, 2012. p. 736–748. <https://doi.org/10.1117/12.926419>.
91. van Holstein RG, Girard JH, De Boer J, Snik F, Milli J, Stam D, Ginski C, Mouillet D, Wahhaj Z, Schmid HM, et al. Polarimetric imaging mode of vlt/sphere/irdis-ii. characterization and correction of instrumental polarization effects. *Astron Astrophys*. 2020;633:64
92. Fusco T, Petit C, Rousset G, Sauvage J-F, Dohlen K, Mouillet D, et al. Design of the extreme AO system for SPHERE, the planet finder instrument of the VLT. *Proc. SPIE 6272, Advances in Adaptive Optics II*, 62720K. 2006. <https://doi.org/10.1117/12.670794>.
93. Fusco T, Sauvage J-F, Petit C, Costille A, Dohlen K, Mouillet D, et al. Final performance and lesson-learned of SAXO, the VLT-SPHERE extreme AO: from early design to on-sky results. *Proc. SPIE 9148, Adaptive Optics Systems IV*, 91481U. 2014. <https://doi.org/10.1117/12.2055423>.
94. Chauvin G, Desidera S, Lagrange A-M, Vigan A, Gratton R, Langlois M, et al. Discovery of a warm, dusty giant planet around HIP 65426. *Astron Astrophys*. 2017;605:9. <https://doi.org/10.1051/0004-6361/201731152>. <https://arxiv.org/abs/1707.01413>

95. Müller A, Keppler M, Henning T, Samland M, Chauvin G, Beust H, et al. Orbital and atmospheric characterization of the planet within the gap of the PDS 70 transition disk. *Astron Astrophys.* 2018;617:2. <https://doi.org/10.1051/0004-6361/201833584>.
96. Milli J, Higon P, Christiaens V, Choquet É, Bonnefoy M, Kennedy GM, et al. Discovery of a low-mass companion inside the debris ring surrounding the F5V star HD 206893. *Astron Astrophys.* 2017;597:2. <https://doi.org/10.1051/0004-6361/201629908>. <https://arxiv.org/abs/1612.00333>
97. Jovanovic N, Martinache F, Guyon O, Clergeon C, Singh G, Kudo T, Garrel V, Newman K, Doughty D, Lozi J, et al. The Subaru coronagraphic extreme adaptive optics system: enabling high-contrast imaging on solar-system scales. *Publ Astron Soc Pac.* 2015;127(955):890.
98. Guyon O, Martinache F, Clergeon C, Russell R, Groff T, Garrel V. Wavefront control with the Subaru coronagraphic extreme adaptive optics (scexao) system. In: *Astronomical Adaptive Optics Systems and Applications IV*, vol. 8149. International Society for Optics and Photonics; 2011. p. 814908.
99. Steiger S, Currie T, Brandt TD, Guyon O, Kuzuhara M, Chilcote J, Groff TD, Lozi J, Walter AB, Fruitwala N, et al. Scexao/mec and charis discovery of a low-mass, 6 au separation companion to hip 109427 using stochastic speckle discrimination and high-contrast spectroscopy. *Astron J.* 2021;162(2):44.
100. Ren D, Dong B, Zhu Y, Christian DJ. Correction of non-common-path error for extreme adaptive optics. *Publ Astron Soc Pac.* 2012;124(913):247. <https://doi.org/10.1086/664947>.
101. Dou J, Ren D. Phase quantization study of spatial light modulator for extreme high-contrast imaging. *Astrophys J.* 2016;832:1–11. <https://doi.org/10.3847/0004-637X/832/1/84>.
102. Gendron E, Assémat F, Hammer F, Jagourel P, Chemla F, Laporte P, Puech M, Marteaud M, Zamkotsian F, Liotard A, Conan J-M, Fusco T, Hubin N. FALCON: multi-object AO. *Compt Rendus Phys.* 2005;6(10):1110–7.
103. Marchetti E, Brast R, Delabre B, Donaldson R, Fedrigo E, Frank C, et al. Mad: practical implementation of mcao concepts. *Compt Rendus Phys.* 2005;6(10):1118–28.
104. Neichel B, Rigaut F. First light for the Gemini Multi-Conjugate Adaptive Optics System. *Spie Newsroom.* 2012. <https://doi.org/10.1117/2.1201201.004101>.
105. Rigaut F, Neichel B, Boccas M, d'Orgeville C, Vidal F, van Dam MA, Arriagada G, Fesquet V, Galvez RL, Gausachs G, et al. Gemini multiconjugate adaptive optics system review–i. design, trade-offs and integration. *Mon Not R Astron Soc.* 2014;437(3):2361–75.
106. Neichel B, Rigaut F, Vidal F, van Dam MA, Garrel V, Carrasco ER, Pessev P, Winge C, Boccas M, d'Orgeville C, et al. Gemini multiconjugate adaptive optics system review–ii. commissioning, operation and overall performance. *Mon Not R Astron Soc.* 2014;440(2):1002–19.
107. Gaessler W, Arcidiacono C, Egner S, Herbst T, Andersen D, Baumeister H, Bizenberger P, Boehnhardt H, Briegel F, Kuerster M, et al. Linc-nirvana: Mcao toward extremely large telescopes. *Compt Rendus Phys.* 2005;6(10):1129–38.
108. Zhang X, Gaessler W, Conrad AR, Bertram T, Arcidiacono C, Herbst TM, Kuerster M, Bizenberger P, Meschke D, Rix H-W, et al. First laboratory results with the linc-nirvana high layer wavefront sensor. *Opt Express.* 2011;19(17):16087–95.
109. Marchetti E, Brast R, Delabre B, Donaldson R, Fedrigo E, Frank C, Hubin N, Kob J, Lizon J-L, Marchesi M, et al. On-sky testing of the multi-conjugate adaptive optics demonstrator. *Messenger* 2007;129:8–13.
110. Marchetti E, Brast R, Delabre B, Donaldson R, Fedrigo E, Frank C, Hubin N, Kolb J, Le Louarn M, Lizon J-L, et al. Mad on-sky results in star oriented mode. In: *Adaptive Optics: Methods, Analysis and Applications*. Optica Publishing Group; 2007. p. 2.
111. Hippler S. Adaptive Optics for Extremely Large Telescopes. *J Astron Instrum.* 2019;8(2):1950001–322. <https://doi.org/10.1142/S2251171719500016>. <https://arxiv.org/abs/1808.02693>
112. van der Luehe O, Soltau D, Berkefeld T, Schelenz T. KAOS: adaptive optics system for the Vacuum Tower Telescope at Teide Observatory. *Proc. SPIE 4853, Innovative Telescopes and Instrumentation for Solar Astrophysics.* 2003. <https://doi.org/10.1117/12.498659>.
113. Berkefeld T, Soltau D, von der Luehe O. Results of the Multi-conjugate Adaptive Optics System at the German Solar Telescope, Tenerife. *Proc. SPIE 5903, Astronomical Adaptive Optics Systems and Applications II*, 59030O. 2005. <https://doi.org/10.1117/12.619132>.
114. Langlois M, Moretto G, Richards K, Hegwer S, Rimmele TR. Solar multiconjugate adaptive optics at the Dunn solar telescope: preliminary results. In: *Advancements in Adaptive Optics, Proceedings of the SPIE, Volume 5490, 2004*. pp. 59–66.
115. Schmidt D, Berkefeld T, Heidecke F, Fischer A, von der Luehe O, Soltau D. GREGOR MCAO looking at the Sun. *Proc. SPIE 9148, Adaptive Optics Systems IV*, 91481T. 2014. <https://doi.org/10.1117/12.2055154>.
116. Goode PR, Denker CJ, Didkovsky LI, Kuhn J, Wang H. 1.6 m solar telescope in big bear-the nst. *J Korean Astron Soc.* 2003;36(spc1):125–33.
117. Langlois M, Moretto G, Béchet C, Montilla I, Tallon M, Goode P, et al. Concept for Solar Multi-Conjugate Adaptive Optics at Big Bear Observatory. 3rd AO4ELT Conference - Adaptive Optics for Extremely Large Telescopes. 62-2013. <https://doi.org/10.12839/AO4ELT3.13316>.
118. Schmidt D, Gorceix N, Goode PR, Marino J, Rimmele T, Berkefeld T, Wöger F, Zhang X, Rigaut F, Von Der Luehe O. Clear widens the field for observations of the sun with multi-conjugate adaptive optics. *Astron Astrophys.* 2017;597:8.
119. Yan J, Zhou R, Yu X. Calculation of the isoplanatic patch for multiconjugate adaptive optics. *Opt Eng.* 1993;32(12). <https://doi.org/10.1117/12.149173>.
120. Yan J, Zhou R, Yu X. Problems with multiconjugate correction. *Opt Eng.* 1994;33(9):2942–4.
121. Ding X, Rong J, Bai H, Wang X, Li F, et al. Theoretical analysis and simulation of conjugate heights for dual-conjugate ao system in lidar. *Chin Opt Lett.* 2008;6(1):1–4.
122. Zhong XC, Wang SJ, Wu YQ. Study of the Conjugate Height for Solar Multi-Conjugate Adaptive Optics. *Applied Mechanics & Materials.* 336-338.1(2013):290-294.
123. Zhong X, Wu Y, Wang S, Huang Z. Deformable mirrors for multi-conjugate solar adaptive optics. *Optik.* 2016;127(2):981–3.

124. Zhong X, Huang Z, Tang T, Wang S. The research on isoplanatic area of double conjugate adaptive optics. *Optik*. 2017;142:119–24.
125. Liu C, Hu L, Cao Z, Mu Q, Xuan L. Modal prediction of atmospheric turbulence wavefront for open-loop liquid-crystal adaptive optics system with recursive least-squares algorithm. *Opt Commun*. 2012;285(3):238–44.
126. Zhang X, Cao Z, Mu Q, Li D, Peng Z, Yang C, Liu Y, Xuan L. Progress of liquid crystal adaptive optics for applications in ground-based telescopes. *Mon Not R Astron Soc*. 2020;494(3):3536–40.
127. Yuan G, Zhao L, Wu P, Wang W. A time-division correction method for adaptive optics system. In: *Journal of Physics: Conference Series*, vol. 2093. IOP Publishing; 2021. p. 012038.
128. Ren D-Q, Zhang X, Liu S-Z. Solar GLAO and TAO: performance comparisons. *Res Astron Astrophys*. 2018;18(7):086. <https://doi.org/10.1088/1674-4527/18/7/86>.
129. Ren D, Zhu Y, Zhang X, Dou J, Zhao G. Solar tomography adaptive optics. *Appl Opt*. 2014;53:1683–96. <https://doi.org/10.1364/AO.53.001683>.
130. Ren D, Jolissaint L, Zhang X, Dou J, Chen R, Zhao G, Zhu Y. Solar ground-layer adaptive optics. *Publ Astron Soc Pac*. 2015;127:000. <https://doi.org/10.1086/681672>.
131. Ren D, Zhang X, Dou J, Zhu Y, Broadfoot R, Chapman J. Pupil-transformation multiconjugate adaptive optics for solar high-resolution imaging. *Opt Eng*. 2016;55:094103. <https://doi.org/10.1117/1.OE.55.9.094103>.
132. Kong L, Zhang L, Zhu L, Bao H, Guo Y, Rao X, Zhong L, Rao C. Prototype of solar ground layer adaptive optics at the 1m new vacuum solar telescope. *Chin Opt Lett*. 2016;14(10):100102.
133. Zhang L, Guo Y, Rao C. Solar multi-conjugate adaptive optics based on high order ground layer adaptive optics and low order high altitude correction. *Opt Express*. 2017;25(4):4356–67. <https://doi.org/10.1364/OE.25.004356>.
134. Rao C, Zhang L, Kong L, Guo Y, Rao X, Bao H, Zhu L, Zhong L, et al. First light of solar multi-conjugate adaptive optics at the 1-m new vacuum solar telescope. *Sci China Phys Mech Astron*. 2018;61:089621.
135. Zhang L, Bao H, Rao X, et al. Ground-layer adaptive optics for the New Vacuum Solar Telescope: Instrument description and first results. *Sci China Phys Mech Astron*. 2023;66:269611. <https://doi.org/10.1007/s11433-022-2107-4>.
136. Gendron E, Vidal F, Brangier M, Morris T, Hubert Z, Basden A, Rousset G, Myers R, Chemla F, Longmore A, et al. Moao first on-sky demonstration with canary. *Astron Astrophys*. 2011;529:2.
137. Andersen DR, Jackson KJ, Blain C, Bradley C, Correia C, Ito M, Lardière O, Véran J-P. Performance modeling for the raven multi-object adaptive optics demonstrator. *Publ Astron Soc Pac*. 2012;124(915):469.
138. Conan R, Bradley C, Lardière O, Blain C, Venn K, Andersen D, et al. Raven: a harbinger of multi-object adaptive optics-based instruments at the Subaru Telescope. *Proc. SPIE 7736, Adaptive Optics Systems II*, 77360T. 2010. <https://doi.org/10.1117/12.856567>.
139. Lardière O, Andersen D, Blain C, Bradley C, Gamroth D, Jackson K, et al. Multi-object adaptive optics on-sky results with Raven. *Proc. SPIE 9148, Adaptive Optics Systems IV*, 91481G. 2014. <https://doi.org/10.1117/12.2055480>.
140. Rigaut F, Rousset G, Kern P, Fontanella J, Gaffard J, Merkle F, Léna P. Adaptive optics on a 3.6-m telescope—results and performance. *Astron Astrophys*. 1991;250:280–90.
141. Rousset G, Beuzit J-L, Hubin NN, Gendron E, Madec PY, Boyer C, et al. Performance and results of the COME-ON+ adaptive optics system at the ESO 3.6-m telescope. *Proc. SPIE 2201, Adaptive Optics in Astronomy*. 1994. <https://doi.org/10.1117/12.176020>.
142. Roddier F. Curvature sensing and compensation: a new concept in adaptive optics. *Appl Opt*. 1988;27(7):1223–5.
143. Wizinowich P, Dekany R, Gavel D, Max C, Adkins S, Bauman B, et al. Wm keck observatory's next generation adaptive optics facility. 2008;7736. <https://doi.org/10.1117/12.790154>
144. Ono YH, Minowa Y, Guyon O, Clergeon CS, Mieda E, Lozi J, et al. Overview of AO activities at Subaru Telescope. *Proc. SPIE 11448, Adaptive Optics Systems VII*, 114480K. 2020. <https://doi.org/10.1117/12.2561139>.
145. Wenhan J. Overview of adaptive optics development. *Opto-Electron Eng*. 2018;45(3):170489–117048915. <https://doi.org/10.12086/oe.2018.170489>
146. Jiang W, Li M, Tang G, Ling N, Li M, Zheng D. Adaptive optical image compensation experiments on stellar objects. *Opt Eng*. 1995;34(1):15–20.
147. Jiang W, Li M, Tang G, Rao C, Ling N, Guan C, et al. Infrared adaptive optics system of the 2.16-m telescope and its wavefront detecting error and performance analysis. *Proc. SPIE 2828, Image Propagation through the Atmosphere*. 1996. <https://doi.org/10.1117/12.254181>.
148. Jiang W, Tang G, Li M, Ling N, Rao C, Guan C, et al. 21-element infrared adaptive optics system at 2.16-m telescope. *Proc. SPIE 3762, Adaptive Optics Systems and Technology*. 1999. <https://doi.org/10.1117/12.363569>.
149. Rao C, Jiang W, Zhang Y, Li M, Ling N, Zhang X, et al. Upgrade on 61-element adaptive optical system for 1.2-m telescope of Yunnan Observatory. *Proc. SPIE 5490, Advancements in Adaptive Optics*. 2004. <https://doi.org/10.1117/12.549402>.
150. Tang G, Rao C, Sheng F, Zhang X, Jiang W. Performance and test results of a 61-element adaptive optics system on the 1.2-m telescope of Yunnan Observatory. *Proc. SPIE 4926, Adaptive Optics and Applications II*. 2002. <https://doi.org/10.1117/12.481678>.
151. Rao C, Jiang W, Zhang Y, Li M, Ling N, Zhang X, et al. Performance on the 61-element upgraded adaptive optical system for 1.2-m telescope of the Yunnan Observatory. *Proc. SPIE 5639, Adaptive Optics and Applications III*. 2004. <https://doi.org/10.1117/12.580415>.
152. Rao C, Jiang W, Zhang Y, Ling N, Zhang X, Xian H, et al. Progress on the 127-element adaptive optical system for 1.8m telescope. *Proc. SPIE 7015, Adaptive Optics Systems*, 70155Y. 2008. <https://doi.org/10.1117/12.787503>.
153. Rao C, Wei K, Zhang X, Zhang A, Zhang Y, Xian H, et al. First observations on the 127-element adaptive optical system for 1.8m telescope. *Proc. SPIE 7654, 5th International Symposium on Advanced Optical Manufacturing and Testing Technologies: Large Mirrors and Telescopes*, 76541H. 2010. <https://doi.org/10.1117/12.866209>.
154. and, and: An active coronagraph using a liquid crystal array for exoplanet imaging: principle and testing. *Res Astron Astrophys*. 2012;12(5):591. <https://doi.org/10.1088/1674-4527/12/5/011>

155. Wang C, hu L, Xu H, Wang Y, Li D, Wang S, Mu Q, Yang C, Cao Z, Lu X, Xuan I, Jiang W, Ling N, Tang G, Li M, Shen F, Rao C, Zhu Y, Xu B. Wavefront detection method of a single-sensor based adaptive optics system. 2015;4. <https://doi.org/10.1364/OE.23.021403-2>
156. Ellerbroek B, Britton M, Dekany R, Gavel D, Herriot G, Macintosh B, Stoesz J. Adaptive optics for the thirty meter telescope. In: *Astronomical Adaptive Optics Systems and Applications II*, vol. 5903. International Society for Optics and Photonics; 2005. p. 590304.
157. Vernin J, Muñoz-Tuñón C, Sarazin M, Ramió HV, Varela AM, Trinquet H, Delgado JM, Fuensalida JJ, Reyes M, Benhida A, et al. European extremely large telescope site characterization i: Overview. *Publ Astron Soc Pac*. 2011;123(909):1334.
158. Johns M, McCarthy P, Raybould K, Bouchez A, Farahani A, Filgueira J, et al. Giant Magellan Telescope: overview. *Proc SPIE 8444, Ground-based and Airborne Telescopes IV*, 84441H. 2012. <https://doi.org/10.1117/12.926716>.
159. Choudhuri AR. Starspots, stellar cycles and stellar flares: Lessons from solar dynamo models. *Sci China Phys Mech Astron*. 2017;60(1):1–16.
160. Low B. Field topologies in ideal and near-ideal magnetohydrodynamics and vortex dynamics. *Sci China Phys Mech Astron*. 2015;58(1):1–20.
161. Wang J, Zhang Y, He H, Chen A, Jin C, Zhou G. Cluster of solar active regions and onset of coronal mass ejections. *Sci China Phys Mech Astron*. 2015;58(9):1–8.
162. Rempel M. Penumbra fine structure and driving mechanisms of large-scale flows in simulated sunspots. *Astrophys J*. 2011;729(1):5.
163. Cao W, Gorceix N, Coulter R, Ahn K, Rimmele T, Goode PR. Scientific instrumentation for the 1.6 m new solar telescope in big bear. *Astronomische Nachr*. 2010;331(6):636–9.
164. Rimmele TR. Solar adaptive optics. In: Wizinowich P.L. (ed.) *Adaptive Optical Systems Technology*, vol. 4007, 2000. p. 218–231. <https://doi.org/10.1117/12.390301>.
165. Rao Changhui Z.L.e.a. Zhu Lei: Development of solar adaptive optics. *Opto-Electron Eng*. 2018;45(3):170733–117073311. <https://doi.org/10.12086/oe.2018.170733>
166. Rimmele TR, Richards K, Hegwer S, Fletcher S, Gregory S, Moretto G, Didkovsky LV, Denker CJ, Dolgushin A, Goode PR, Langlois M, Marino J, Marquette W. First results from the NSO/NJIT solar adaptive optics system. In: Fineschi S, Gummin MA (eds.) *Telescopes and Instrumentation for Solar Astrophysics*, vol. 5171, 2004. p. 179–186. <https://doi.org/10.1117/12.508513>.
167. Didkovsky L, Dolgushyn A, Marquette W, Nenow J, Varsik J, Goode P, Hegwer S, Ren D, Fletcher S, Richards K, Rimmele T, Denker C, Wang H. High-order adaptive optical system for big bear solar observatory. *Proc SPIE - Int Soc Opt Eng*. 2003;4853:630–9. <https://doi.org/10.1117/12.471341>.
168. Shumko S, Gorceix N, Choi S, Kellere A, Cao W, Goode P, Abramenco V, Richards K, Rimmele T, Marino J. Ao-308: The high-order adaptive optics system at big bear solar observatory, vol. 9148, 2014. p. 914835. <https://doi.org/10.1117/12.2056731>
169. Hardy JW. Solar Imaging Experiment: Final Report, Feb. 1979 – Jun. 1980, AFGL-TR-80-0338. Lexington, MA: Air Force Geophysics Laboratory, Hanscom AFB; 1980. (Cited on page 19).
170. Rimmele TR, Radick RR. Solar adaptive optics at the National Solar Observatory. In: Bonaccini D, Tyson RK (eds.) *Adaptive Optical System Technologies*. Society of Photo-Optical Instrumentation Engineers (SPIE) Conference Series, vol. 3353, 1998. p. 72–81. <https://doi.org/10.1117/12.321734>
171. Schmidt W, von der Lühe O, Volkmer R, Denker C, Solanki SK, Balthasar H, Bello González N, Berkefeld T, Collados Vera M, Hofmann A, Kneer F, Lagg A, Puschmann KG, Schmidt D, Sobotka M, Soltau D, Strassmeier KG. The GREGOR Solar Telescope on Tenerife. In: Rimmele TR, Tritschler A, Wöger F, Collados Vera M, Socas-Navarro H, Schlichenmaier R, Carlsson M, Berger T, Cadavid A, Gilbert PR, Goode PR, Knölker M (eds.) *Second ATST-EAST Meeting: Magnetic Fields from the Photosphere to the Corona*. Astronomical Society of the Pacific Conference Series, vol. 463, 2012. p. 365. <http://arxiv.org/abs/1202.4289>
172. Berkefeld T, Soltau D, von der Luhe OFH. Second-generation adaptive optics for the 1.5 m solar telescope GREGOR, Tenerife. *Proc SPIE 5490, Advancements in Adaptive Optics*. 2004. <https://doi.org/10.1117/12.555505>.
173. Berkefeld T, Schmidt D, Soltau D, Lühe O, Heidecke F. The gregor adaptive optics system. *Astronomische Nachr*. 2012;333:863. <https://doi.org/10.1002/asna.201211739>.
174. Berkefeld T, Schmidt D, Soltau D, Heidecke F, Fischer A. The adaptive optics system of the 1.5m GREGOR solar telescope: four years of operation. *Proc SPIE 9909, Adaptive Optics Systems V*, 990924. 2016. <https://doi.org/10.1117/12.2232604>.
175. Asensio Ramos A, de la Cruz Rodríguez J, Pastor Yabar A. Real-time, multiframe, blind deconvolution of solar images. *A A*. 2018;620:73. <https://doi.org/10.1051/0004-6361/201833648>.
176. Denker C, Tritschler A, Rimmele TR, Richards K, Hegwer SL, Wöger F. Adaptive optics at the big bear solar observatory: Instrument description and first observations. *Publ Astron Soc Pac*. 2007;119(852):170–82. <https://doi.org/10.1086/512493>.
177. Rimmele TR, Warner M, Keil SL, Goode PR, Knölker M, Kuhn JR, et al. The Daniel K. Inouye Solar Telescope - Observatory Overview. *Sol Phys*. 2020;295(12):172. <https://doi.org/10.1007/s11207-020-01736-7>
178. Chang-HuiRao, Wen-HanJiang, ChengFang, NingLing, Wei-ChaoZhou, Ming-DeDing, Xue-JunZhang, Dong-HongChen, meiLi, Xiu-FaGao: A tilt-correction adaptive optical system for the solar telescope of nanjing university. *Res Astron Astrophys*. 2003;(6).
179. Rao C-h, Jiang W-h, Ling N, Beckers JM. Tracking algorithms for low-contrast extended objects. *Chin Astron Astrophys*. 2002;26(1):115–24. [https://doi.org/10.1016/S0275-1062\(02\)00049-8](https://doi.org/10.1016/S0275-1062(02)00049-8).
180. Rao C, Zhu L, Rao X, Guan C, Chen D, Lin J, Liu Z. 37-element solar adaptive optics for 26-cm solar fine structure telescope at yunnan astronomical observatory. *Chin Opt Lett*. 2010;8(10):966–8.
181. Rao C-H, Zhu L, Rao X-J, Zhang L-Q, Bao H, Ma X-A, Gu N-T, Guan C-L, Chen D-H, Wang C, et al. First generation solar adaptive optics system for 1-m new vacuum solar telescope at fuxian solar observatory. *Res Astron Astrophys*. 2016;16(2):003.

182. Rao C, Zhu L, Rao X, Zhang L, Bao H, Kong L, Guo Y, Zhong L, Li M, Wang C, et al. Instrument description and performance evaluation of a high-order adaptive optics system for the 1 m new vacuum solar telescope at fuxian solar observatory. *Astrophys J*. 2016;833(2):210.
183. Rao C, Gu N, Rao X, Li C, Zhang L, Huang J, Kong L, Zhang M, Cheng Y, Pu Y, Bao H, Guo Y, Liu Y, Yang J, Libo Z, Wang C, Fang K, Zhang X, Chen D, Ma W. First light of the 1.8-m solar telescope-clst. *Sci China Phys Mech Astron*. 2020;63. <https://doi.org/10.1007/s11433-019-1557-3>
184. Johns M, McCarthy P, Raybould K, Bouchez A, Farahani A, Filgueira J, Jacoby G, Shectman S, Sheehan M. Giant Magellan Telescope: overview. In: Stepp LM, Gilmozzi R, Hall HJ (eds.) *Ground-based and Airborne Telescopes IV*. Society of Photo-Optical Instrumentation Engineers (SPIE) Conference Series, vol. 8444, 2012. p. 84441. <https://doi.org/10.1117/12.926716>
185. Ellerbroek B. The TMT Adaptive Optics Program.
186. Busoni L, Agapito G, Plantet C, Oberti S, Verinaud C, Le Louarn M, et al. Adaptive optics design status of maory, the mcao system of European elt. 2020. <https://doi.org/10.48550/arXiv.2012.14626>.
187. Rimmele T, Hegwer S, Marino J, Richards K, Schmidt D, Waldmann T, Woeger F. Solar multi-conjugate adaptive optics at the dunn solar telescope. In: Array (ed.) *1st AO4ELT Conference - Adaptive Optics for Extremely Large Telescopes*, 2010. p. 08002. <https://doi.org/10.1051/ao4elt/201008002>.
188. Quintero Noda C, Schlichenmaier R, Bellot Rubio LR, Löfdahl MG, Khomenko E, Jurcak J, Leenaarts J, Kuckein C, González Manrique SJ, Gunar S, Nelson CJ, de la Cruz Rodríguez J, Tziotziou K, Tsiropoula G, Aulanier G, Collados M, the EST team: The European Solar Telescope. 2022. <http://arxiv.org/abs/2207.10905>
189. Berkefeld T. The ao and mcao for the 4m european solar telescope, 2017. <https://doi.org/10.26698/AO4ELT5.0173>
190. Wu Y, Guo Y, Bao H, Rao C. Sub-millisecond phase retrieval for phase-diversity wavefront sensor. *Sensors*. 2020;20(17):4877.
191. Guo Y, Wu Y, Li Y, Rao X, Rao C. Deep phase retrieval for astronomical Shack-Hartmann wavefront sensors. *Mon Not R Astron Soc*. 2022;510(3):4347–54.
192. Liu X, Morris T, Saunter C, de Cos Juez FJ, González-Gutiérrez C, Bardou L. Wavefront prediction using artificial neural networks for open-loop adaptive optics. *Mon Not R Astron Soc*. 2020;496(1):456–64. <https://doi.org/10.1093/mnras/staa1558>.

Publisher's Note

Springer Nature remains neutral with regard to jurisdictional claims in published maps and institutional affiliations.